Small Molecule Inhibition of Quiescin Sulfhydryl Oxidase 1 (QSOX1), a Dynamic Pro-

Tumorigenic Regulator of the Extracellular Matrix

by

Paul D. Hanavan

A Dissertation Presented in Partial Fulfillment
of the Requirements for the Degree
Doctor of Philosophy

Approved November 2015 by the
Graduate Supervisory Committee:

Douglas Lake, Chair
Joshua LaBaer
Marco Mangone
Chad Borges

ARIZONA STATE UNIVERSITY

December 2015

ABSTRACT

Quiescin sulfhydryl oxidase 1 (QSOX1) is a highly conserved disulfide bond-generating enzyme that represents the ancient fusion of two major thiol-disulfide oxidoreductase gene families: thioredoxin and ERV. QSOX1 was first linked with cancer after being identified as overexpressed in pancreatic ductal adenocarcinoma (but not in adjacent normal ductal epithelia, infiltrating lymphocytes, or chronic pancreatitis). QSOX1 overexpression has been confirmed in a number of other histological tumor types, such as breast, lung, kidney, prostate, and others. Expression of QSOX1 supports a proliferative and invasive phenotype in tumor cells, and its enzymatic activity is critical for promoting an invasive phenotype. An *in vivo* tumor growth study utilizing the pancreatic tumor cell line MIAPaCa-2 containing a QSOX1-silencing shRNA construct revealed that QSOX1 expression supports a proliferative phenotype. These preliminary studies suggest that suppressing the enzymatic activity of QSOX1 could represent a novel therapeutic strategy to inhibit proliferation and invasion of malignant neoplasms.

The goal of this research was to identify and characterize biologically active small molecule inhibitors for QSOX1. Chemical inhibition of QSOX1 enzymatic activity was hypothesized to reduce growth and invasion of tumor cells. Recombinant QSOX1 was screened against libraries of small molecules using an enzymatic activity assay to identify potential QSOX1 inhibitors. Two lead QSOX1 inhibitors were confirmed, 2-phenyl-1, 2-benzisoselenazol-3-one (ebselen), and 3-methoxy-n-[4-(1 pyrrolidinyl)phenyl]benzamide. The biological activity of these compounds is consistent with QSOX1 knockdown in tumor cell lines, reducing growth and invasion *in vitro*. Treatment of tumor cells with

i

these compounds also resulted in specific ECM defects, a phenotype associated with QSOX1 knockdown. Additionally, these compounds were shown to be active in pancreatic and renal cancer xenografts, reducing tumor growth with daily treatment. For ebselen, the molecular mechanism of inhibition was determined using a combination of biochemical and mass spectrometric techniques. The results obtained in these studies provide proof-of-principle that targeting QSOX1 enzymatic activity with chemical compounds represents a novel potential therapeutic avenue worthy of further investigation in cancer. Additionally, the utility of these small molecules as chemical probes will yield future insight into the general biology of QSOX1, including the identification of novel substrates of QSOX1.

DEDICATION

I am fortunate to have a close group of people in my life who strongly supported my decision to go to graduate school and rode this wave with me through (sometimes) rough waters. It would have been impossible to achieve half of what I have without them. To my mother Denise Hanavan, and my father John Hanavan. To my aunt, Keli Shea. I love you all and owe you everything.

To the love of my life, Joe Gallego.

To Maggie.

To Dana Bernson for her devoted friendship, and her late husband Jon Bernson – you are missed. To my friend Ben Katchman, whose pioneering work in QSOX1 during his graduate studies set the stage for my success, and whose free therapy and personal training sessions helped keep my mind and body healthy.

Most of all, though, this work is dedicated to the memory of my sister Lauren Hanavan, whose long and difficult battle with juvenile diabetes pissed me off enough to want to make a difference. This is for you, Laur.

ACKNOWLEDGMENTS

Thank you to all current and former members of the Lake Lab and the excellent undergraduates I have been fortunate enough to train, including Kirsten Ward and Amber Fifield. Thank you to Cheryl Myers, whose friendship and professional discussions meant a great deal in and out of the lab. Last, but certainly not least, thank you to Yvette Ruiz. The trove of knowledge and skills you possess easily surpasses most people. Thank you for teaching me everything you know, making me into a good laboratory citizen, and for being a good friend for many years.

TABLE OF CONTENTS

LIST OF TABLES

# LIST OF FIGURES

CHAPTER 1

INTRODUCTION

Oxidative protein folding is a critical process in all cells, responsible for the introduction of structural disulfide bonds in proteins as well as maintenance of cellular redox homeostasis [1]. Without proper pairing of thiols in proteins to form disulfide bonds, proteins would not assume a structure that allows them to correctly function. Thiol oxidations are performed by a wide variety of enzymes including protein disulfide isomerases (PDI), thiol-disulfide oxidoreductases and various chaperone proteins [2]. Due to the strongly reducing nature of the cytoplasm favoring the persistence of thiols [3], disulfide bond formation is typically (though not always [4]) relegated to more oxidative environments such as the endoplasmic reticulum (ER) and mitochondrial intermembrane [5]. In the ER, PDI acts in conjunction with ER oxidoreductase 1 (Ero1) to accomplish the tasks of disulfide formation and thiol-disulfide exchange reactions [6, 7]. In reduced proteins, PDI oxidizes sulfhydryls in client substrates via a redox-active CXXC motif in its thioredoxin (Trx) domain [8], transferring electrons to Ero1 through disulfide exchange, which ultimately completes the redox cycle via the reduction of molecular oxygen by its bound FAD cofactor [6]. Thus the generation of disulfide bonds by PDI and sulfhydryl oxidases like Ero1 requires their coordinated function.

Quiescin sulfhydryl oxidases (QSOX), by contrast, are a unique class of enzymes that can complete the entire oxidative cycle of disulfide formation through intramolecular electron transfer. QSOX's, of which there are two members in humans (QSOX1 and SOXN/QSOX2[9]), are characterized by the ancient fusion (>1 billion years ago) of Trx

1

and 'essential for respiration and vegetative growth' (ERV) [10], a yeast mitochondrial sulfhydryl oxidase similar to the mammalian 'augmenter of liver regeneration' (ALR) [11, 12]. QSOX1, the most widely studied quiescin sulfhydryl oxidase is highly conserved; it is expressed in all eukaryotic multicellular organisms analyzed and several protists including those of the genus Trypanosoma [13], but not in fungi [10]. QSOX1 contains an active amino-terminal thioredoxin-like domain with the canonical CXXC motif characterized by the thioredoxins (Figure 1); it also contains a second, degenerate, thioredoxin domain that does not contribute to its redox activity. The sulfhydryl oxidase ERV portion of the enzyme contains two CXXC motifs and the FAD cofactor [14]. Given its dynamic modular structure, QSOX is the only class of enzyme capable of *de novo* disulfide generation and intramolecular disulfide transfer. QSOX1 has two major isoforms, a long (747 a.a.) form (QSOX1-L) that contains a transmembrane domain, and a short form (604 a.a.) generated from alternative splicing. QSOX1 is localized to the golgi apparatus, ER, and in secretory vesicles, but it has been demonstrated that both isoforms are secreted and are potentially dimerized [15].

QSOX1 was initially discovered as a gene upregulated as fibroblasts exit the proliferative cycle and enter reversible quiescence [10]. It was rapidly recognized as a secreted enzyme active extracellularly; QSOX1 is found in chicken egg white [16, 17] and in conditioned medium from fibroblasts [18]. However, QSOX1 does have intracellular activity, capable of reversing the lethality of a total knockout of Ero1 when ectopically expressed in yeast [19].

The biochemical mechanisms underlying QSOX1 enzymatic activity are well-studied [13, 14, 19-29]. Similar to PDI, the CXXC motif (C70-C73) in the first thioredoxin domain oxidizes reduced substrates, followed by intramolecular transfer of electrons to the FAD-proximal CXXC (C459-C462) in the ERV domain [26]. This transfer is facilitated by a conformational change that brings the thioredoxin and ERV domains into close proximity [20, 21]. Electron transfer between the thioredoxin and ERV CXXC motifs is promoted by a mixed disulfide intermediate that creates a charge transfer complex with FAD, overcoming thermodynamic barriers that would otherwise disfavor the electron transfer [24]. While a third CXXC in the ERV domain (C519-C522) was once proposed to be involved in the catalytic cycle of human QSOX1 based on studies utilizing avian QSOX1 [26], molecular and biochemical studies have shown that it is not required in the human QSOX1 disulfide relay system [23, 29].

While the enzymology of QSOX1 activity is well-characterized, its biological functions are poorly understood. An early study reported that QSOX1 protects cells against the induction of apoptosis after cellular exposure to Fe(III)-hydroxyquinoline or hydrogen peroxide, and is upregulated in response to such treatments [30]. QSOX1 expression was also induced in Nkx3.1-deficient hyperplastic prostatic epithelia and prostatic intraepithelial neoplasias lacking Nkx3.1 (but not cells with normal morphology lacking this tumor suppressor), suggesting a role for QSOX1 in the development of prostate cancer [31].

The link between QSOX1 and cancer was further strengthened by the detection of a peptide from QSOX1-L in plasma from patients with pancreatic ductal

adenocarcinoma, but absent in healthy donor plasma [32]. Staining of matched pancreatic adenocarcinoma and normal adjacent tissue microarrays with a QSOX1 antibody showed strong expression of QSOX1 in tumor cells but not in normal ductal epithelia and surrounding non-malignant stroma [33]. The same study detected robust QSOX1 expression in pancreatic tumor cell lines by Western blotting, demonstrating a link between a circulating antigen from QSOX1 with its overexpression in pancreatic ductal adenocarcinoma.

Following up on the overexpression of QSOX1 in pancreas cancer, Katchman and colleagues adopted a "hallmarks of cancer [34]" approach to characterize the cellular biology of QSOX1 as it relates to tumorigenic processes. Using shRNA-mediated suppression of QSOX1 protein in pancreatic tumor cell lines, QSOX1 was shown to promote a proliferative and invasive phenotype *in vitro* [35]. Furthermore, QSOX1 expression was associated with increased activation of matrix metalloproteinases (MMPs) -2 and -9 [35], proteolytic enzymes involved in degradation of the basement membrane during tumor cell invasion [36]. The induction of QSOX1 expression by hypoxia-inducible factor-1 (HIF-1) was demonstrated to promote the invasion of pancreatic tumor cells; this effect was inhibited by QSOX1 silencing, supporting the crucial role of QSOX1 in mediating invasion [37].

These studies were expanded to breast cancer, showing a similarly increased rate of growth and invasive activity in breast tumor cell lines overexpressing QSOX1 [38]. Importantly, this study also identified the enzymatic activity of QSOX1 as critical to the pro-invasive effect of QSOX1, evidenced by rescue of the invasive phenotype after

addition of exogenous enzymatically active, but not inactive, recombinant QSOX1 (rQSOX1). Analysis of the Gene Expression-Based Outcome for Breast Cancer Online (GOBO) database revealed that patients diagnosed with the luminal B subtype of breast cancer whose tumors expressed elevated QSOX1 levels had significantly poorer relapse free and overall survival than luminal B patients whose tumors expressed low levels of QSOX1. QSOX1 expression is also associated with higher tumor grades [38]. The overexpression of QSOX1 in breast cancer and its association with advanced tumor grade is corroborated by a serial analysis of gene expression (SAGE) analysis of cDNAs derived from clinical samples of breast cancer [39]. One conflicting study, however, links overexpression of QSOX1 in breast cancer cell lines with reduced growth and invasion as well as improved clinical prognosis [40]. These results are in direct conflict with the findings of Katchman et. al [38], but analysis of the composition of their clinical samples casts doubt on their data [41]. While a consensus is building in support of the pro-growth and invasive properties of QSOX1 in cancer, additional research is warranted to clarify this discrepancy.

The composition of the extracellular matrix (ECM) is recognized to play a major role in the regulation of normal cellular functions [42, 43], and modulation of the ECM by cancer cells may enhance tumorigenesis [44]. Since QSOX1 is a secreted catalyst of disulfide bond formation whose activity has been shown to affect the structure of the ECM [35], identification of its extracellular substrates has important implications in our understanding of the normal and pathological role of ECM dynamics. A recent study identified laminin α4 as substrate for QSOX1 whose incorporation into the ECM was

defective in cells with reduced QSOX1 expression through shRNA-mediated knockdown [45]. α4 laminins are associated with an invasive phenotype in cancer and decreased adhesion [46, 47], linking a demonstrated QSOX1 substrate with increased tumor aggression. Loss of QSOX1 increases the concentration of ECM sulfhydryls [45], demonstrating a rich source of potential novel substrates.

With mounting evidence supporting a pro-tumorigenic role for QSOX1 whose enzymatic activity is required for its invasive and extracellular modulatory activities, it was hypothesized that inhibition of QSOX1 has anti-tumorigenic effects with important clinical significance. Early work to address this hypothesis has shown promising results. Small molecule inhibition of QSOX1 by the glutathione peroxidase mimic ebselen, for example, was shown to have *in vitro* and *in vivo* activity in tumor cells consistent with QSOX1 knockdown including growth inhibition, suppression of invasion, and a reduction in tumor size in nude mouse xenografts [48]; these results are discussed in depth in Chapter 3. Other groups have taken a different approach. A single-chain antibody directed against the thioredoxin 1 domain of QSOX1, for example, was shown to inhibit enzymatic activity and invasion of a lung tumor cell line across a fibroblast monolayer [22]. Another group has explored the potential for arsenic-based compounds in inhibition oxidative protein folding by QSOX1 and PDI chemotherapeutically, but reports non-specificity in their preference for free cysteines [49]. The development of specific inhibitors for QSOX1 is therefore required to elucidate the effectiveness of chemical targeting of QSOX1 versus antibody-based inhibition in a clinical setting.

6

The goal of this research was to identify and characterize small molecule inhibitors for QSOX1 as lead compounds for eventual clinical utility. It was hypothesized that a chemical compound capable of inhibiting the enzymatic activity of QSOX1 would decrease the growth and invasion of tumor cells and modulate ECM structure and function, consistent with *in vitro* observations. Using a cell-free activity assay, rQSOX1 was screened against two small molecule libraries in collaboration with Sanford Burnham Prebys Medical Discovery Institute, identifying 24 potential inhibitors. Of these, 2 compounds (2-phenyl-1, 2-benzisoselenazol-3-one (ebselen), and 3-methoxy-n-[4-(1-pyrrolidinyl)phenyl]benzamide) (SBI-183), were shown to both inhibit QSOX1 and growth inhibitory properties. In the subsequent chapters, the biological and biochemical characterization of these molecules are discussed.
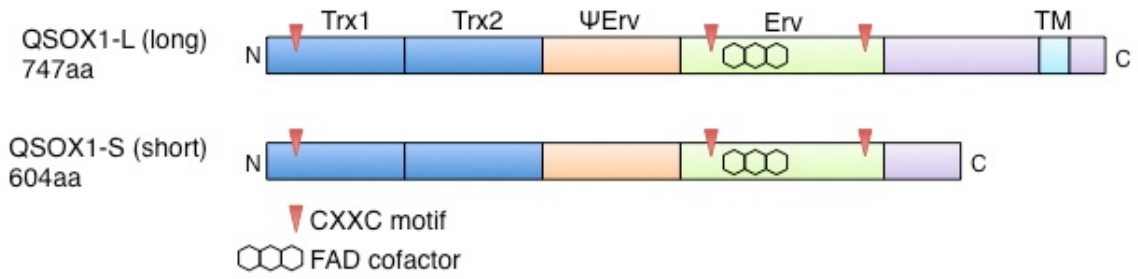
**Figure 1**. Structure of QSOX1. QSOX1-L (top) and QSOX1-S (bottom) shown. Thioredoxin domains shown in blue. ERV domain shown in green with the location of the FAD cofactor represented by three hexagons representing the isoalloxazine ring. CXXC motifs shown as inverted red triangles. Not to scale.

CHAPTER 2

METHODS TO CHARACTERIZE SMALL MOLECULE INHIBITORS FOR QSOX1

**Overview:**

In collaboration with Sanford Burnham Prebys Medical Discovery Institute, rQSOX1 was screened against two small molecule libraries: the Library of Pharmacologically Active Compounds (LOPAC[1280]) and an in-house 50,000 compound library, utilizing a RNAse A substrate-based cell-free activity assay. Hits identified in this screen were confirmed using a homovanilic acid activity assay with a DTT substrate, and then subjected to a biological screen to identify compounds with growth inhibitory effects. Mass spectrometry, molecular, and biochemical assays were utilized to determine the mechanism of inhibition of QSOX1. Tumor cell lines were treated with compounds, and their effects on the growth of tumor cell lines and invasion were quantified compared to vehicle controls. Nude mice were implanted with tumor cell line xenografts and then treated with compounds to determine their effects on tumor growth compared to control mice. Compounds were also analyzed for their effects on modulation of the extracellular matrix through sulfhydryl quantitation and defects in laminin incorporation.

**Materials and methods:**

*Cell culture.*

All cells were cultured in a humidified incubator at 37 °C with 5% $CO_2$. Media was supplemented with 5% fetal bovine serum (Gibco, Carlsbad, CA USA) and 100

9

μg/ml penicillin/streptomycin (Gibco)  Pancreatic tumor cell lines MIAPaCa-2 and BXPC3 were maintained in Dulbecco's Modified Eagle Medium (DMEM), (Gibco). Renal cancer cell line 786-O was cultured in RPMI 1640 (MediaTech, Manassas, VA USA). Renal cancer cell line UOK117 was cultured in DMEM, supplemented with 1X MEM nonessential amino acids (Mediatech). Peripheral blood mononuclear cells (PBMC) were isolated from whole blood from a normal donor in accordance to an approved IRB protocol using Ficol-Paque (GE Healthcare) and maintained in Iscove's Modified Dulbecco's Medium (IMDM, MediaTech). All cells were passaged regularly at a confluency of 70% and all experiments were performed using sub-confluent cultures. 786-O cells were cultured from frozen stocks purchased from Sigma-Aldrich and were authenticated by STR analysis after thawing. UOK117 cells were received from the Linehan laboratory at the National Cancer Institute and experiments performed from early passage stocks. MIAPaCa-2 and BXPC3 cells were cultured from frozen stocks that underwent independent STR testing 12/2012.

*QSOX1 knockdown.*

Lentiviruses packaged with short hairpin RNA (shRNA) constructs specific for human QSOX1 (sh528, sh742) or a nonspecific scrambled sequence (shScr) were produced in 293T cells as reported by Katchman et al. [35]. Knockdown of QSOX1 in MIAPaCa-2 was confirmed by western blotting using anti-QSOX1 antibody (Protein Tech, Chicago, IL USA).

*Nude mouse-human tumor xenograft model.*

Stably transduced MIAPaCa-2 cells (shScr, sh742, and sh528) were harvested

from subconfluent cultures after brief exposure to Cell Stripper (Corning, Corning NY).

Cell suspensions were counted, washed once in ice cold serum-free RPMI and

resuspended in cold 1xPBS. $2.4 \times 10^7$ total cells were mixed in a 1:1 ratio with Matrigel

(BD Biosciences) according to manufacturer specifications. Cells were kept on ice

throughout the procedure. Female athymic $Foxn1^{nu}$ mice (Harlan, Indianapolis, IN USA)

were injected with $1 \times 10^6$ MIAPaCa-2 cells in Matrigel. Mice were housed in a barrier

facility on HEPA-filtered racks. All experiments were conducted with strict adherence to

aseptic technique and IACUC regulations. Each mouse was subcutaneously injected with

$200\mu l$ of cell suspension into the right hind flank using a 21-gauge needle. Mice were

examined every other day to determine the volume of the tumor using calibrated calipers.

Real-time tumor volume was measured as $V = 0.5 \times length \times width^2$. When the tumors

reached a volume of 1500-2000 $mm^3$ the mice were sacrificed and the tumor was excised,

measured and weighed.

For ebselen treatment of nude mice, three groups were tested: 1) 20% DMSO

(vehicle), 2) 160 µg/day ebselen, and 3) 640 µg/day ebselen. 160 and 640 µg ebselen

represent an equivalent dose of 150mg and 600mg for a 70 kg human, respectively. $1 \times 10^6$

MIAPaCa-2 cells were injected subcutaneously into each mouse as before, and tumors

were allowed to grow for 3 days. Ebselen was then administered once daily through oral

gavage for 28 days. Real-time tumor volume was determined through caliper

measurement of tumors over the course of the study [50]. Error is represented as SEM.

Statistical significance was determined using two-way analysis of variance (ANOVA), comparing drug-treated with vehicle-treated mice. Corrections for multiple comparisons were made using Dunnett's Test.

For renal cancer xenografts treated with SBI-183, 6-8 week female nude mice were injected subcutaneously with $1\times10^6$ UOK117 or 786-O cells in a 100 μl 1:1 matrigel:SFM suspension in the right hind flank using a 23 gauge needle (n =5 x 3 groups). Mice were monitored daily for tumor growth and, 7 days after injection, daily oral gavage of SBI-183 was begun. Mice received 400 μg (100 μl) of SBI-183, dissolved in DMSO vehicle to a concentration of 13.5 mM, or 100 μl DMSO vehicle every 24 hours. Tumors were also measured in a group that did not receive treatment. Regular caliper measurements were taken, measuring the length, width, and depth of growing tumors. Real-time tumor volume was monitored as stated previously. At the conclusion of the study, mice were euthanized by $CO_2$ asphyxiation, weighed, and tumors excised for histological analysis. Insufflated lungs, livers, and the adjacent inguinal lymph nodes were also saved. All tissues were fixed in 10% formalin for 48 hours, and preserved in 70% ethanol.

*rQSOX1 expression and purification.*

rQSOX1 was produced and purified according to the method of Heckler [23]. Rosetta-gami B (DE3) cells (Novagen, Billerica MA USA) were transformed with 50 ng pET15b containing truncated QSOX1-S. The rQSOX1 construct contains an N-terminal poly-histidine tag and encodes amino acids 33-546 of QSOX1-S. The activity of the

recombinant enzyme verified as described below using a dithiothreitol (DTT) substrate [25]. The elution profile for rQSOX1 and MALDI/LC-MS$^2$ analysis of trypsin-digested rQSOX are shown in Figures 2 and 3, respectively.

*rQSOX1 small molecule screen.*

A HTS assay was developed using reduced denatured RNAse A substrate [51]. Hydrogen peroxide produced in the QSOX1 reaction was detected using ROS-Glo kit (Promega, Madison WI) as a primary assay and HyPerBlu (Lumigen, Southfield MI) as a secondary assay per manufacturers instructions. Assays were optimized and reaction kinetic parameters were determined. The assays were miniaturized to final volume of 2 uL. HTS was also performed using the ROS-Glo assay with a substrate concentration of 80 uM RNAse A (that is close to $K_m$ value of 122 μM). rQSOX1 protein was utilized at 10 nM concentration, >20-fold over the limit of assay detection yet still on the linear portion of the enzyme-dependent activity. rQSOX1 was screened against compounds from the LOPAC$^{1280}$ library (Sigma-Aldrich, St. Louis MO USA) at 12.5 μM compound concentration, or an "in-house" 50,000 compound library at Sanford Burnham Prebys Medical Discovery Institute. Compounds that demonstrated >50% inhibition were re-tested using single-concentration in triplicate wells, followed by concentration-dependent confirmation in the primary and secondary QSOX1 assays. A luminescent assay for glucose oxidase (GOx) was used as a counter-screen. The GOx assay utilizing glucose as a substrate was detected using ROS-Glo. Active and selective compounds were

13

purchased in dry powder form, dissolved in DMSO and reconfirmed in the assays before use in the confirmatory assays utilizing the GOx counter-screen.

*rQSOX1 activity assay*.

The sulfhydryl oxidase activity of rQSOX1 was confirmed using DTT and RNAse A substrates and a fluorogenic hydrogen peroxide indicator, homovanilic acid (HVA) [25]. In this assay, 150 nM rQSOX1 was added to 600 $\mu$M thiols from reduced DTT or RNAse A, 1 mM HVA, 1.4 $\mu$M HRP, and 300 $\mu$M EDTA in PBS at 25 $^{\circ}$C, pH 7.5. Assays were performed in black 96-well plates with a final reaction volume of 150 $\mu$l. Fluorescence signal was measured over 10 minutes at $\lambda_{ex}$ 320 nm and $\lambda_{em}$ 420 nm using a FlexStation spectrophotometer (Molecular Devices, Sunnyvale CA USA). Readings were taken in 20 second intervals after the addition of rQSOX1. Ebselen was added to reactions at least 10 minutes prior to the addition of rQSOX1 at concentrations ranging from 250 nM – 4 $\mu$M.

Results for the HVA-based activity assay for rQSOX1 and ebselen are shown in Figure 5.

*Compounds*.

2-phenyl-1,2-benzisoselenazol-3(2H)-one (MW = 274.18 g/mol), ebselen (Sigma-Aldrich), was dissolved in tissue culture-grade DMSO (Sigma-Aldrich, St. Louis, MO.) to a stock concentration of 10 mM and stored at -20 °C protected from light. 3-methoxy-N-[4-(1-pyrrolidinyl)phenyl]benzamide ("SBI-183," MW = 296 g/mol) was purchased

14

from ChemBridge Corp. (San Diego CA). Compound stocks were dissolved in tissue culture-grade DMSO (Sigma-Aldrich) at a concentration of 10 mM for *in vitro* studies, and 13.5 mM for *in vivo* studies.

*Growth kinetics of ebselen-treated tumor cells.*

$1\times10^4$ cells/well MIAPaCa-2, BXPC3, 786-O, and UOK1117 were plated in duplicate in 24-well plates. Cells were adhered overnight prior to the addition of fresh media (untreated), vehicle (0.15% DMSO), or 5 μM – 15 μM ebselen. Cells were counted using a hemacytometer and Trypan Blue exclusion to assess viability. Cells were counted on days 3 and 5, and "floaters" (disadhered and dead cells) were saved for determination of overall viability. Media was replaced on day 3 for the 5$^{th}$ day time point; floaters were saved and added back to each well for counting on day 5. Viability was determined as [1-(# dead cells / (# live cells + # dead cells))*100]. Error is represented as the standard error of the mean. Significance was determined using paired T-testing for each time point compared to vehicle-treated cells.

*Trans-well invasion assays.*

$2\times10^4$ MIAPaCa-2, BXPC3, 786-O, or UOK117 cells were seeded in rehydrated 24-well invasion assay inserts containing 8 μm pores overlaid with Matrigel (Corning) in serum-free media; cells were adhered for 1 hour prior to addition of ebselen, SBI-183, or vehicle. Inserts were incubated in wells containing complete media for 20 hours at 37 $^{o}$C. Non-invading cells were removed with cotton swabs and membranes were fixed with 100

% methanol and mounted on slides with DAPI (Life Technologies). The total number of invading cells was determined by manual counting of DAPI-stained nuclei.

*Electrospray Ionization Mass Spectrometry.*

2 μM rQSOX1 was incubated with 20 μM ebselen (10-fold excess) with or without 10 mM DTT substrate (added 5 minutes prior to mass analysis). For SBI-183 studies, 12 pmol rQSOX1 was incubated with vehicle or 5 μM SBI-183. Samples ere analyzed intact by liquid chromatography-electrospray ionization-mass spectrometry (LC-ESI-MS) on a Dionex Ultimate 3000 HPLC equipped with a 1:100 flow splitter connected to a Bruker Maxis 4G quadrupole-time-of-flight (Q-TOF) mass spectrometer. A trap-and-elute form of LC-MS was carried out in which 15 μL samples were loaded at 10 μl/min in 80/20 water/acetonitrile containing 0.1% formic acid (loading solvent) onto a Bruker-Michrom protein captrap configured for bi-directional flow on a 6-port diverter valve. The trap was then rinsed with the HPLC loading pump at 10 μl/min for 40 min to completely remove PBS buffer salts. The flow over the captrap was then switched to the micropump, set at 2 μL/min, and ramped over 5 minutes from 80% water containing 0.1% formic acid (Solvent A) / 20% acetonitrile (Solvent B) to 90% acetonitrile and held for 3 min.

The captrap eluent was directed to the mass spectrometer operating in positive ion, TOF-only mode, acquiring spectra in the *m/z* range of 300 to 3000 with a nominal resolving power of ~60,000 m/Δm FWHM. ESI settings for the Agilent G1385A capillary microflow nebulizer ion source were as follows: End plate offset -500 V, capillary -3500 V, nebulizer nitrogen 2 bar, dry gas nitrogen 3.0 L/min at 225 °C. Data

were acquired in profile mode at a digitizer sampling rate of 4 GHz. Spectra rate control was by summation at 1 Hz.

rQSOX1 eluted over a period of about 1 minute; under the above conditions, rQSOX1 ranged in charge state from +32 to +60. Raw mass spectra were averaged across this timeframe, baseline subtracted and charge deconvoluted with Bruker DataAnalysis 4.1 charge deconvolution software to a mass range of 1000 Da on either side of any identified peak.


*Maleimide protection assay*.

2 μM rQSOX1 in 1X PBS (pH 7.5) was incubated with a 5-fold molar excess of ebselen or vehicle for 5 minutes at 25 °C. AlexaFluor488-C5-maleimide (Life Technologies, Carlsbad CA) was added to a final concentration of 100 μM. Reactions were incubated for 30 minutes at 37°C, protected from light. Protein from each reaction was resolved on 12% polyacrylamide gels in non-reducing conditions. Gels were washed twice for 5 minutes in ddH$_2$O and imaged under UV light. Gels were then stained with Coomassie R-250 for 15 minutes. Band intensities were analyzed by ImageJ, and are represented as "percent signal" of rQSOX1 pre-incubated with vehicle.


*Cyanylation and ammonia-based cleavage at free cysteines*.

Free cysteines on rQSOX1 were identified by treatment of recombinant enzyme with the sulfhydryl cyanylating reagent 1-Cyano-4-dimethylaminopyridinium tetrafluoroborate (CDAP) followed by ammonia-mediated N-terminal cleavage and

analysis by MALDI-MS [52]. 100 pmol rQSOX1 was dissolved in 0.1 M citrate containing 6 M guanidine-HCl, pH 3.0. CDAP was added to a concentration of 25 mM from a freshly prepared 200 mM stock and incubated for 15 minutes at 25 $^{\circ}$C. Trifluoroacetic acid (TFA) was added to a concentration of 0.2%, and protein was purified using C18 ZipTips (Millipore); purified rQSOX1 was eluted with 90% ACN with 0.1% TFA in MilliQ $H_2O$. Samples were dried and reconstituted in 6 M guanidine-HCl containing 1 M $NH_4OH$, pH 11.5. Samples were incubated for 60 minutes at 37 $^{\circ}$C. Reactions were quenched by reducing the pH to 3.0 with citric acid. Disulfide bonds were reduced in 100 mM TCEP dissolved in ddH2O for 30 minutes at 37 $^{\circ}$C. 0.2% TFA was added, and C18 ZipTip purification was repeated as before. Samples were eluted with 3 ul 90 % ACN/0.1 % TFA directly onto MALDI targets; 2 µl saturated sinapinic acid in 33% ACN/0.4 % TFA was added and samples air-dried.

*MALDI Mass Spectrometry.*

Masses of cyanylation/ammonia-induced protein cleavage products of rQSOX1 were determined by MALDI-MS on a Bruker Ultraflex-III MALDI mass spectrometer equipped with a Nd:YAG laser operating in positive-ion, delayed extraction linear mode, with ion source 1 at 25.00 kV, ion source 2 at 23.10 kV, lens at 7.50 kV, 150 ns delay, and 1 GS/s sample rate. Prior to acquisition of the mass spectra, the target mass range was externally calibrated using a mixture of calibrants obtained from Bruker Daltonics (Billerica, MA USA).

*SBI-183 dose response*.

5x10$^3$ 786-O or UOK117 cells, 1x10$^4$ HDFn, or 1x10$^5$ PBMC were plated in triplicate in 96-well tissue culture-treated plates the day before compound addition. 40 μM – 39 nM SBI-183 in complete media appropriate for each cell type was added and plates incubated for 48 hours in a humidified incubator. For PBMC, cells were tested with or without the addition of 10 μg/ml phytohemagglutinin (PHA) to stimulate T-cell proliferation. Media was replaced with 100 μl/well 50 μg/ml 3-(4,5-dimethylthiazol-2-yl)-2,5-diphenyltetrazolium bromide (MTT) in phenol red-free media. Cells were incubated for 4 hours and lysed with 100 mg/ml sodium dodecyl sulfate (SDS) in 0.01M hydrochloric acid (HCl). Plates were incubated for 18 hours and the absorbance measured at 570 nm.

*SBI-183 proliferation assay*.

2.5x10$^3$ 786-O or UOK117 cells per well were plated in a 96-well plates in complete media and allowed to adhere overnight. Media was replaced with complete media containing 10 μM  5 μM SBI-183, or vehicle (0.15% DMSO); each condition was performed in triplicate. 2 hours after addition of SBI-183 or vehicle, one plate for each cell line was used in an MTT assay to determine baseline absorbance ("Day 0"). Remaining plates were incubated in a humidified incubator, and MTT assays were performed at days 3 and 5 after the addition of SBI-183. Media was replaced at day 3 due to evaporation.

*Extracellular matrix sulfhydryl quantitation.*

$5\times10^3$ 786-O or $7.5\times10^3$ UOK117 cells per well were plated in 96-well plates and

allowed to adhere overnight. The following day, media was replaced with ebselen, SBI-

183 or vehicle-containing complete media and cells were incubated for 48 hours in a

humidified incubator. Media was removed and plates were washed once with 1X PBS

containing 1 mM EDTA. 50 μl 1% Triton X-100, 5 mM $NH_4OH$ in 1X PBS was added to

wells and placed on a titer plate shaker for 30s to de-roof the cell monolayer and expose

the ECM. To all wells that received SBI-183 (n=6 per concentration of compound) and

one set of vehicle wells (n=6), 50 μl of 6 μM maleimide-$PEG_2$-biotin (Molecular Probes)

in 1X PBS (freshly made) was added. Remaining vehicle wells received either 100 mM

dithiothreitol (DTT) or 100 μM N-ethyl maleimide (NEM) as a positive and negative

control (n=6 per treatment). Plates were incubated with controls for 2 hours on titer plate

shaker (all following incubation steps were performed on shaker); all wells were then

washed twice with PBS/EDTA followed by the addition of 50 μl of 6 μM maleimide-

$PEG_2$-biotin to control wells and 150 μl blocking buffer (1% BSA in 1X PBS). Plates

were incubated for 2 additional hours. Control wells were washed twice and 150 μl

blocking buffer was added per well; plates were incubated for 2 hours. Blocking buffer

was replaced with 50 μl/well 1:10,000 streptavidin conjugated to horseradish peroxidase

(HRP) in blocking buffer, and plates were incubated for 2 hours. Plates were washed 6

times for 2 minutes each wash in 1X PBS containing 0.05% Tween-20. 100 μl/well

3,3',5,5'-Tetramethylbenzidine (TMB) substrate (BD, Franklin Lakes, NJ) was added per

well and after sufficient color development 50 μl/well 2N $H_2SO_4$ was added to quench the reaction. Absorbance was measured at 490nm.

*Immunofluorescence.*

1x10$^4$ cells/ml 786-O or UOK117 were plated in wells of a 24-well plate each containing a class coverslip pre-coated with poly L-lysine. Cells were adhered overnight, and media was replaced with complete media containing SBI-183 or DMSO vehicle. Cells were incubated for 48 hours. Coverslips were washed with 1X PBS, and then fixed in 250 μl/well 2% paraformaldehyde (PFA) in 1XPBS at RT. Cells were washed once with PBS, and permeabilized for 1 hour in 1% Triton X-100 in 1X PBS with gentle rocking. Coverslips were washed twice with PBS for 5 minutes with gentle rocking. Coverslips were then blocked with 1% BSA in 1X PBS for 1 hour at room temperature with gentle rocking. Primary antibodies in blocking buffer were added as follows and incubated overnight rocking gently at 4$^o$C: 1:200 rabbit anti-LAMA4 (Novus, Littleton CO), 1:200 rabbit anti-LAMA2 (Novus). Coverslips were washed 3 times for 5 minutes each in 1X PBS on rocker, and 1:500 goat anti-rabbit conjugated to AlexaFluor 488 (Molecular Probes) was added and coverslips were incubated, rocking, for 2 hours protected from light. 4 washes, 10 minutes each in PBS, were performed. Coverslips were then mounted in DAPI-containing mounting media (Life Technologies).
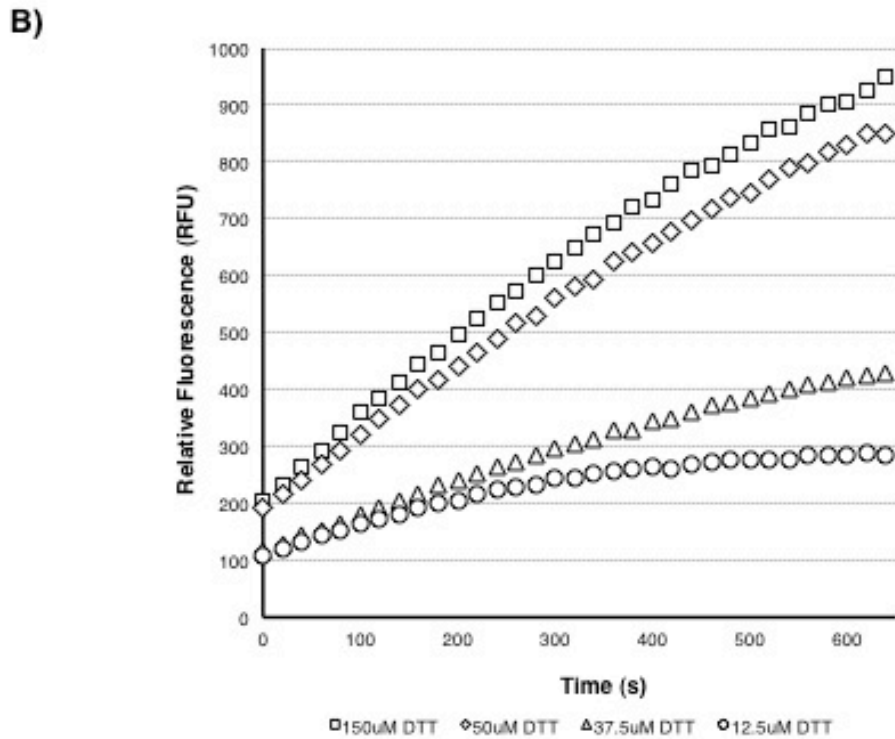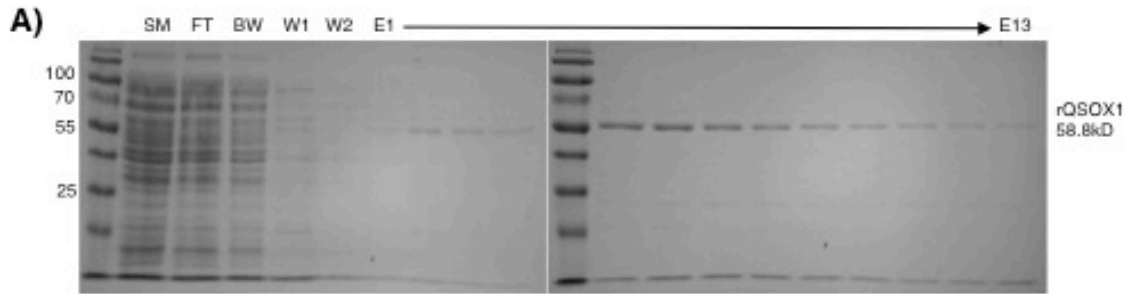
**Figure 2.** Purification of active rQSOX1  A) Elution profile of rQSOX1. SM = starting material (lysate), FT = NI-NTA column flowthrough, BW = binding buffer wash, W1 = wash #1, W2 = wash #2, E1-E13 = elution fractions. B) Activity of rQSOX1 reacted with varying DTT substrate concentrations. As described in methods section, 150 uM, 50 uM, 37.5 uM, and 12.5 μM DTT was used in HVA-based activity assays with 150 nM rQSOX1. Total relative fluorescence was monitored over a 10 minute period.

22

Sequence coverage of trypsin-digested rQSOX1 (MALDI):
**MGHHHHHHHMSALYSPSDPLTLLQADTVR**GAVLGSRSAWAVEFFASW<u>C</u>GH<u>C</u>IAFAPTWK
ALAEDVKAWRPALYLAALDCAEETNSAVCR**DFNIPGFPTVR**FFKAFTKNGSGAVFPVAG
ADVQTLRERLIDALESHHDTWPPA(C)PPLEPAK**LEEIDGFFARNNEEYLALIFEK**GGS
YLAREVALDLSQHKGVAVRR**VLNTEANVVRK**FGVTDFPS(C)YLLFRNGSVSR**VPVLME**
**SRSFYTAYLQR**LSGLTREAAQTTVAPTTANK**IAPTVWK**LADR**SKIYMADLESALHYILR**
**IEVGRFPVLEGQR**LVALKKFVAVLAK**YFPGRPLVQNFLHSVNEWLKRQKRNKIPYSFFK**
TALDDRKEGAVLAK**KVNWIGCQGSEPHFR**GFPCSLWVLFHFLTVQAARQNVDHSQEAAK
**AKEVLPAIR**GYVHYFFG<u>C</u>RD<u>C</u>ASHFEQMAAASMHR**VGSPNAAVLWLWSSHNRVNARLAG**
**APSEDPQFPK**VQWPPREL<u>C</u>SA<u>C</u>HNER**LDVPVWDVEATLNFLKAHFSPSNIILDFPA**

Sequence coverage of trypsin-digested rQSOX1 (Orbitrap, LC-MS/MS):
MGHHHHHHHMSALYSPSDPLTLLQADTVRGAVLGSRSAWAVEFFASW<u>C</u>GH<u>C</u>IAFAPTWK
**ALAEDVK**AWRPALYLAALDCAEETNSAVCR**DFNIPGFPTVRFFKAFTKNGSGAVFPVAG**
**ADVQTLR**ERLIDALESHHDTWPPA(C)PPLEPAK**LEEIDGFFARNNEEYLALIFEK**GGS
YLAR**EVALDLSQHKGVAVRRVLNTEANVVRK**FGVTDFPS(C)YLLFRNGSVSR**VPVLME**
**SRSFYTAYLQRLSGLTREAAQTTVAPTTANKIAPTVWKLADR**SK**IYMADLESALHYILR**
**IEVGRFPVLEGQRLVALKKFVAVLAK**YFPGRPLVQNFLHSVNEWLKRQKR**NKIPYSFFK**
**TALDDRKEGAVLAKK**VNWIGCQGSEPHFRGFPCSLWVLFHFLTVQAAR**QNVDHSQEAAK**
**AKEVLPAIR**GYVHYFFG<u>C</u>RD<u>C</u>ASHFEQMAAASMHR**VGSPNAAVLWLWSSHNRVNARLAG**
**APSEDPQFPKVQWPPR**EL<u>C</u>SA<u>C</u>HNER**LDVPVWDVEATLNFLK**AHFSPSNIILDFPA

**Figure 3.** Mass spectral analysis of trypsin-digested rQSOX1. Peptides identified from A) MALDI, or B) LC-MS/MS analysis are bolded and underlined. Underlined (but not bolded) residues represent redox-active C-X-X-C motifs. Cysteines in parentheses, C165 and C237, were identified as ebselen-binding cysteines (Figure 12).

23

CHAPTER 3

EBSELEN INHIBITS QSOX1 ENZYMATIC ACTIVITY AND SUPPRESSES

INVASION OF PANCREATIC AND RENAL CANCER CELL LINES

Hanavan PD, Borges CR, Katchman BA, Faigel DO, Ho TH, Ma CT, Sergienko EA, Meurice N, Petit JL, Lake DF: **Ebselen inhibits QSOX1 enzymatic activity and suppresses invasion of pancreatic and renal cancer cell lines**. Oncotarget 2015, 6:18418-18428.

**Overview:**

Quiescin sulfhydryl oxidase 1 (QSOX1) is a highly conserved disulfide bond-generating enzyme that is overexpressed in diverse tumor types. Its enzymatic activity promotes the growth and invasion of tumor cells and alters extracellular matrix composition. In a nude mouse- human tumor xenograft model, tumors containing shRNA for QSOX1 grew significantly more slowly than controls, suggesting that QSOX1 supports a proliferative phenotype *in vivo*. High throughput screening experiments identified ebselen as an *in vitro* inhibitor of QSOX1 enzymatic activity. Ebselen treatment of pancreatic and renal cancer cell lines stalled tumor growth and inhibited invasion through Matrigel *in vitro*. Daily oral treatment with ebselen resulted in a 58% reduction in tumor growth in mice bearing human pancreatic tumor xenografts compared to controls. Mass spectrometric analysis of ebselen-treated QSOX1 mechanistically revealed that C165 and C237 of QSOX1 covalently bound to ebselen. This report details the anti-neoplastic properties of ebselen in pancreatic and renal cancer cell lines. The results here offer a "proof-of-principle" that enzymatic inhibition of QSOX1 may have clinical relevancy.

**Results:**

*QSOX1 expression drives increased tumor growth in vivo.*

Suppression of QSOX1 levels in tumors expressing shRNAs specific for QSOX1 was hypothesized to slow their growth compared to controls, based on the results of *in vitro* studies. Tumors containing QSOX1 shRNAs (sh742 or sh528) grew at a reduced rate compared to shScr control and untreated MIAPaCa-2 xenografts (Figure 4A). Tumor masses on day 28 of the experiment showed that tumor growth was reduced by 77% in tumors transduced with sh742, and by 48% in tumors transduced with sh528 compared to shScr tumors (Figure 4B, C). These results indicate that QSOX1 expression promotes tumor growth *in vivo* and suggest that QSOX1 could be a target for potential anti-neoplastic compounds.

*Ebselen inhibits rQSOX1 activity in vitro.*

A sulfhydryl activity assay similar to the one developed by Colin Thorpe's group [25] was used to screen recombinant QSOX1 against a library of pharmacologically active compounds, LOPAC[1280]. In this enzymatic assay (Figure 5A), rQSOX1 oxidizes a reduced RNAse A or DTT substrate, producing $H_2O_2$ detected by a luminescent reaction. In the presence of a QSOX1 inhibitor, the sulfhydryl oxidase activity of QSOX1 is blocked, preventing disulfide bond formation and $H_2O_2$ production. The relative inhibitory activity of LOPAC[1280] is plotted in Figure 5B. Ebselen (Figure 5C) was identified as an inhibitor of QSOX1 enzyme activity, with greater inhibitory activity against QSOX1 than GOx (Figure 5D); the $IC_{50}$ for ebselen inhibition of QSOX1 and

25

GOx was determined to be 5.4 μM and 20.5μM, respectively. Confirmation of ebselen's inhibitory activity was obtained by HyPerBlu luminescent detection (Figure 5D, middle plot) and HVA-based fluorescent assays showing decreased fluorescence as inhibitor concentration increases (Figure 6).

*Ebselen reduces tumor cell invasion.*

One of the fundamental properties of malignant cells leading to metastatic disease is invasion. Since ebselen inhibits QSOX1, it was hypothesized that ebselen would suppress invasion of tumor cells similar to shRNA-mediated knockdown of QSOX1.

MIAPaCa-2, BXPC3, 786-O, and UOK117 cells were incubated in matrigel-coated invasion chambers in serum-free media in the presence of ebselen or vehicle. Invading cells were quantified after 20 hours (Figure 7). Isogenic MIAPaCa-2 lines were generated that express shRNAs specific for QSOX1 (sh742 and sh528) or a nonspecific sequence (shScr) (Figure 7A). shScr cells exposed to 5 μM – 15 μM ebselen showed decreased invasion compared to DMSO vehicle-treated cells, with reductions of 91%, 94%, and 98%, respectively. sh742 cells showed greater than 60% decreased invasion compared to shScr cells. Invasion was rescued to levels of vehicle-treated shScr wells when 50 nM active rQSOX1 was added to sh742 wells at the initiation of the assay (Figure 7A, sixth bar). rQSOX1 pre-incubated with 15 μM ebselen and then added to sh742 cells, however, did not rescue invasion. These results suggest that one of the mechanisms by which ebselen suppresses invasion is through QSOX1 inhibition.

Invasion was quantified for ebselen-treated BXPC3, 786-O, and UOK117 cells

(Figure 7B-D). Ebselen suppressed invasion in these tumor cell lines in a concentration-

dependent manner. At 5 μM, BXPC3 invasion was reduced by 85%, 89% for 786-O, and

40% for UOK117. 10 μM ebselen treatment decreased BXPC3, 786-O, and UOK117

invasion by 95%, 97%, and 80% compared to vehicle-treated cells, respectively. Near

total inhibition of invasion was observed for each cell line treated with 15 μM ebselen.

These results were statistically significant in BXPC3 and UOK117 with p-values

calculated at <0.05. Results for 786-O were not statistically significant (p = 0.08 – 0.09),

but show a similar dose-response.


*Ebselen reduces tumor growth in vivo.*

Nude mice subcutaneously injected with MIAPaCa-2 cells were treated for 28

days with ebselen by oral gavage at two clinically achievable doses to determine if

ebselen suppresses tumor growth *in vivo*. As shown in Figure 8, daily treatment with

ebselen at both high (640 μg) and low (160 μg) doses suppressed tumor growth in

MIAPaCa-2 nude mouse xenografts. There was no difference in tumor size between high

and low doses, but tumors in mice treated with 160 μg ebselen were ~56% smaller than

vehicle-treated mice at day 28. There was no difference in the average masses of mice

between the vehicle and ebselen-treated groups (Figure 9), suggesting that the observed

difference in tumor growth were not due decreased appetite or decreased nutrient

absorption in ebselen-treated mice. Taken together, these results suggest that ebselen

decreases tumor growth *in vivo*.

*Ebselen leads to increased ECM sulfhydryls and defects in laminin α4 deposition.*

It was recently demonstrated that QSOX1 is required for the successful integration of specific laminin subunits into the extracellular matrix [45]. Suppression of QSOX1 expression causes an increases in sulfhydryls – QSOX1 substrates – in the ECM. Whether QSOX1 inhibition by ebselen resulted in these phenotypes was explored. $1x10^4$ MIAPaCa-2 cells were grown in the presence or absence of ebselen for a period of 48 hours, and de-roofed the cell monolayer to expose the ECM. Wells were then treated with maleimide-$PEG_2$-biotin and the relative quantity of sulhydryls present were quantified with SA-HRP and a TMB substrate. A significant increase in sulfhydryls from ebselen-treated cells was observed, representing a 40% increase compared to vehicle-treated cells (Figure 10A).

The effect of ebselen treatment on the deposition of laminin α4 (an established QSOX1 substrate) in the extracellular matrix of 786-O cells was determined . $1x10^4$ cells/ml were plated on poly-L lysine-coated wells and subjected to ebselen or vehicle treatment for a period of 48 hours. Cells were then fixed and stained with anti-laminin α4 antibodies and imaged. A marked decrease in laminin present in the ECM of ebselen-treated cells was observed compared to vehicle-treated cells (Figure 10B), suggesting that inhibition of QSOX1 by ebselen led to the defective processing of this laminin chain. These results further strengthen previous results that ebselen inhibition of QSOX1 leads to functional defects associated with QSOX1 activity.

*Ebselen covalently binds to QSOX1.*

Ebselen is reactive with reduced cysteines through the formation of a Se-S bond
with target sulfhydryls [53]. It was therefore hypothesized that ebselen covalently binds
with cysteines in QSOX1, which would suggest a mechanism for the inhibition of
enzymatic activity. The formation of ebselen adducts would be expected to increase the
mass of QSOX1 by the molecular weight of one or more ebselen molecules, 274.18 Da.
LC-MS analysis was performed on untreated or ebselen-treated rQSOX1 in the presence
or absence of DTT (an established substrate for QSOX1) [16, 22, 25] (Figure 11).
Untreated rQSOX1 (Figure 11A, top spectrum) displays two prominent peaks with
masses of 58 683 and 58 860 Da, designated "A" and "B," respectively, corresponding to
two post-translationally modified forms of rQSOX1.

Treatment of QSOX1 with ebselen shows a mass shift corresponding to two
ebselen adducts per peak (Figure 11A, middle spectrum). In the bottom spectrum of
Figure 11A, rQSOX1 was also treated with ebselen in the presence of DTT substrate. The
masses of unmodified rQSOX and rQSOX1 containing 1 or 2 ebselen molecules were
detected simultaneously, suggesting that DTT can remove ebselen from QSOX1.

A protection assay based on the sulfhydryl specificity of maleimide was used to
determine the cysteine preference of ebselen (Figure 11B), blocking free cysteines in
QSOX1 with ebselen pre-treatment followed by incubation with the thiol-reactive
compound maleimide. Vehicle-treated rQSOX1 showed strong fluorescence at the
expected MW of 58.8 kDa, but ebselen pre-treatment decreased resting QSOX1

fluorescence by >94%. These results suggest that ebselen binds to free cysteines in resting QSOX1.

*Identification of ebselen-binding cysteines in QSOX1.*

A cyanylation strategy was employed to identify ebselen-binding cysteines in resting QSOX1, utilizing the reagent 1-cyano-4-dimethylaminopyridinium tetrafluoroborate (CDAP). CDAP cyanylates free, but not disulfide-bound, cysteines in proteins; they are then cleaved on the amino side of the CDAP-cysteine adduct when subjected to alkaline conditions [54-57]. MALDI analysis of CDAP-treated, cleaved and reduced rQSOX1 revealed 3 unique cleavage fragments (Figure 12A). Fragments 1, 2, and 3 had observed masses of 15 668, 8 063.1, and 35 242 Da, respectively (black arrows in Figure 12A). These masses correspond to cleavage with the expected iminothiazolidine formation [54-57] on the N-terminal side of cysteines 165 and 237 in QSOX1 as shown in the diagram in Figure 12B. Predicted versus observed molecular weights for these cleavage products are shown in Figure 12C. The cyanyl group increases fragment masses by 25 Da (fragments 2 and 3).
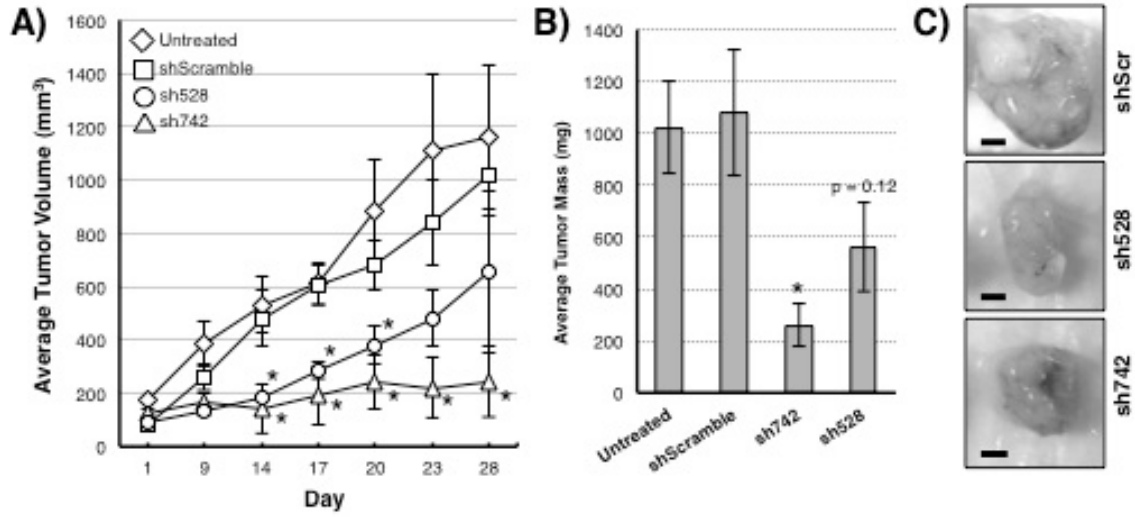
**Figure 4.** Growth of MIAPaCa-2 tumors in nude mice. A) Growth kinetics of MiaPaca-2 tumors with QSOX1 knockdowns (sh742 triangles, sh528 circles), scrambled control (squares), or untreated (diamonds); n = 5 mice per group. B) Final tumor masses on day 28. C) Images of shScr (top), sh528 (middle), or sh742 (bottom) tumors dissected from mice on day 28. Significance was determined by T-test; knockdowns were compared to vehicle-treated tumors. *p<0.05. Bar = 3mm.
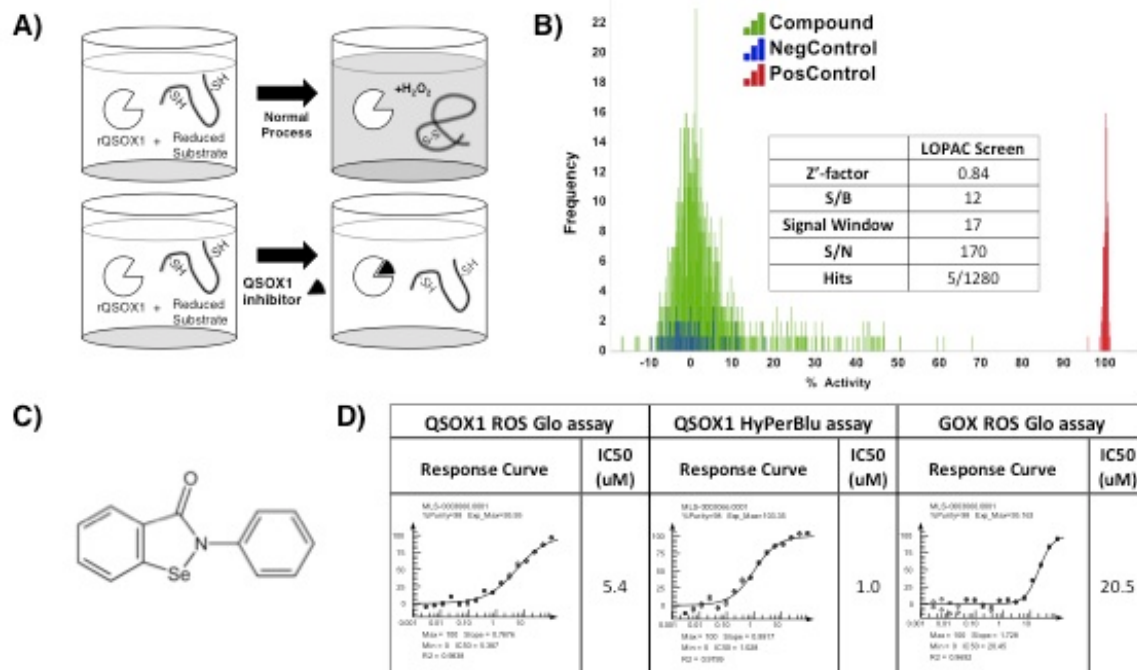
**Figure 5.** High-throughput screen for QSOX1 inhibitors using LOPAC[1280] identified ebselen as a QSOX1 inhibitor. A) Diagram of QSOX1 sulfhydryl oxidase activity reaction used in high-throughput screening and HVA activity assays. B) Distribution plot with primary HTS data showing positive (red bars) and negative (blue bars) controls, and compounds (green bars) at 12.5 μM concentration. Inset table summarizes plate statistics for HTS campaign. C) Structure of ebselen. D) Concentration-dependent inhibition curves for ebselen for QSOX1 (ROS Glo left, HyPerBlu middle) and GOx (ROS Glo right).

32
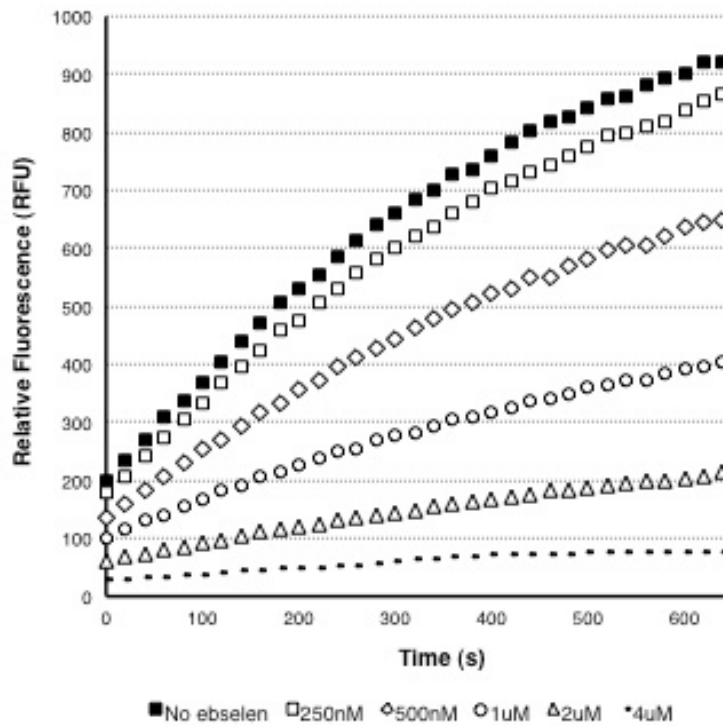
**Figure 6.** Relative activity of 150 nM rQSOX1 with 300 μM DTT substrate in the presence of 250 nM – 4 μM ebselen. Ebselen was added to reactions at least 10 minutes prior to rQSOX1 addition. Reactions were monitored over a period of 10 minutes.
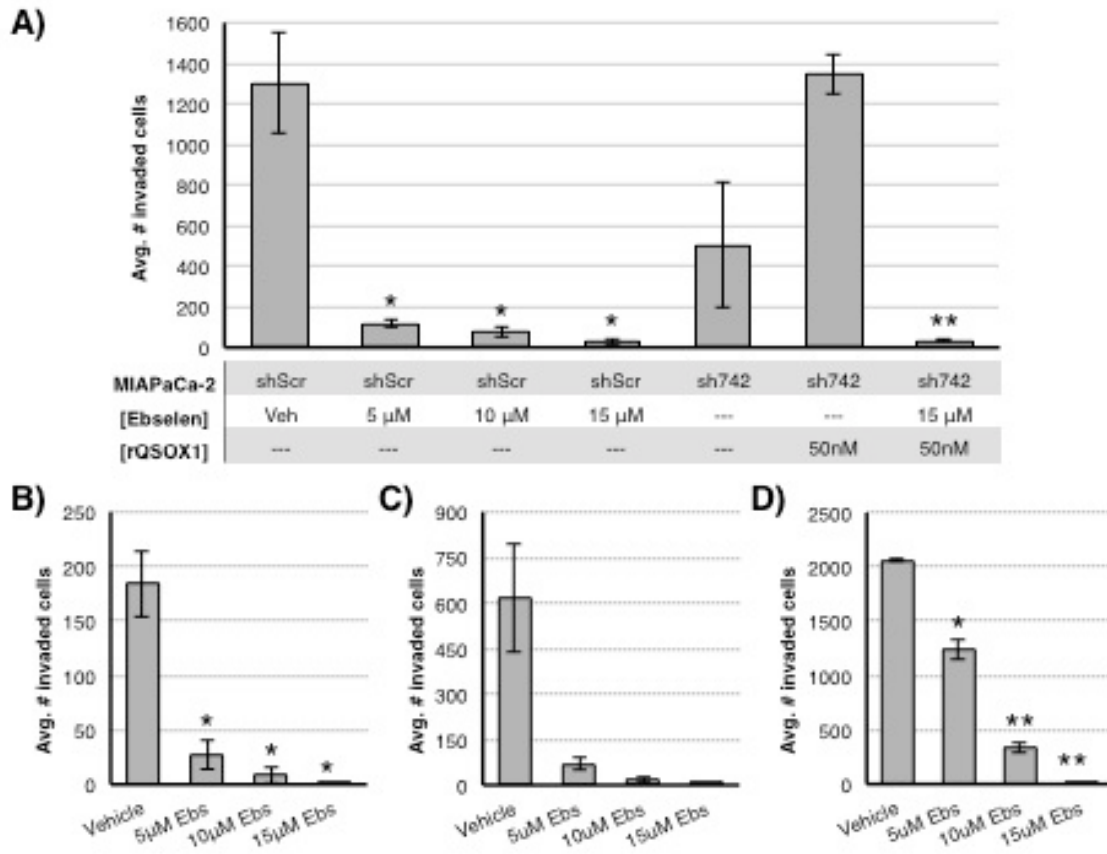
**Figure 7.** Ebselen inhibits invasion of pancreatic and renal cell cancer cell lines through a Matrigel basement membrane. A) Isogenic MIAPaCa-2 cell lines transduced with a QSOX1-specific shRNA (sh742) or a nonspecific sequence (shScr) were incubated for 20 hours in invasion well inserts; cells were exposed to 5-15uM ebselen or vehicle +/- 50 nM rQSOX1 (sh742 only). Invasion of B) BXPC3, C) 786-O, and D) UOK117 cells exposed to ebselen or vehicle. Vehicle was 0.15% DMSO. Error bars represent SEM. For (A), significance for ebselen-treated shScr cells was calculated for vehicle-treated shScr cells. For sh742 cells, significance is relative to sh742 cells treated with rQSOX1 alone. n = 3 fields averaged for all conditions. Statistical significance was determined by T-test. *p < 0.05, **p<0.01.
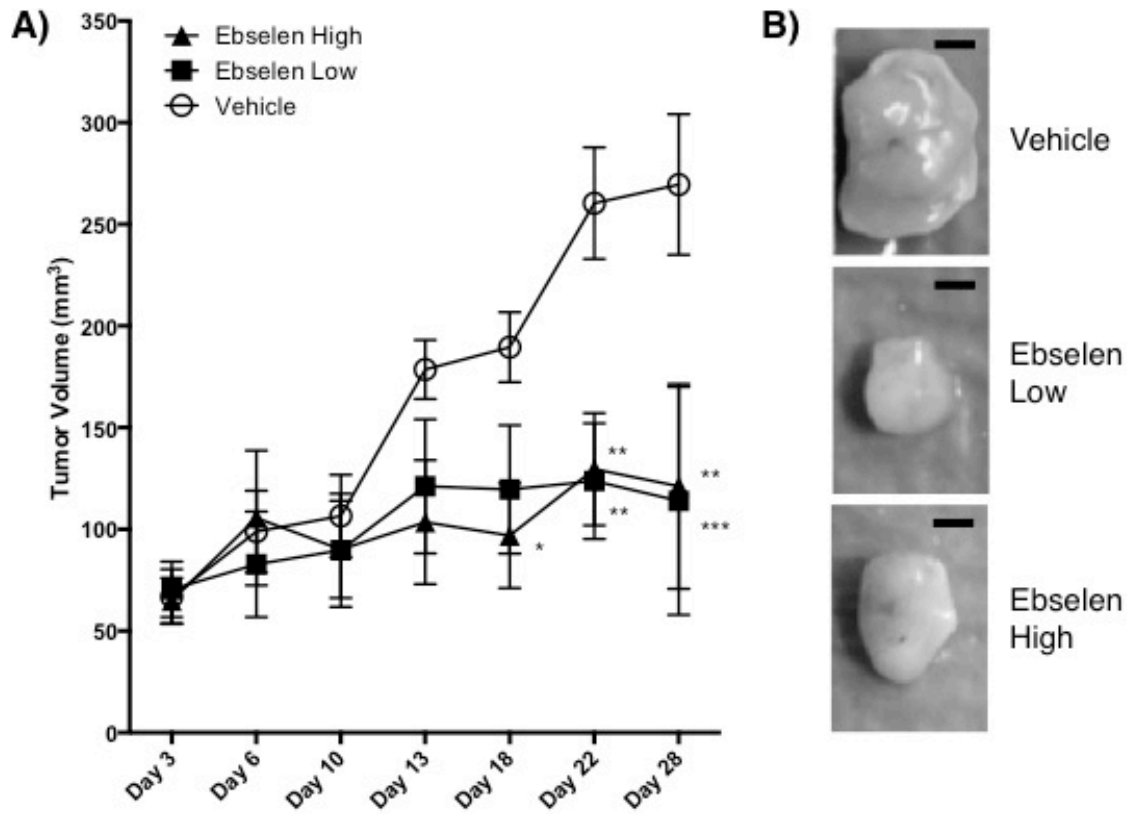
**Figure 8.** Ebselen treatment of nude mice bearing human tumors. A) One million MIAPaCa2 cells were mixed with Matrigel and used to inoculate nude mice (5 mice/group) on day 0. Mice were gavaged daily starting on day 3 with vehicle (20% DMSO, open circle), 160 µg/day ebselen (filled square) or 640 µg/day ebselen (filled triangle) in DMSO. Tumor measurements are shown for days 3, 6, 10, 13, 18, 22 and 28. Tumor volume is shown on the Y-axis and time in days is shown on the X-axis. Significance was determined by two-way ANOVA with Dunnet's Test used to correct for multiple comparisons compared to vehicle-treated mice. * ($p < 0.05$), ** ($p < 0.01$), *** ($p < 0.001$). B) Representative tumors from vehicle-treated and ebselen-treated mice. Bar = 2mm.
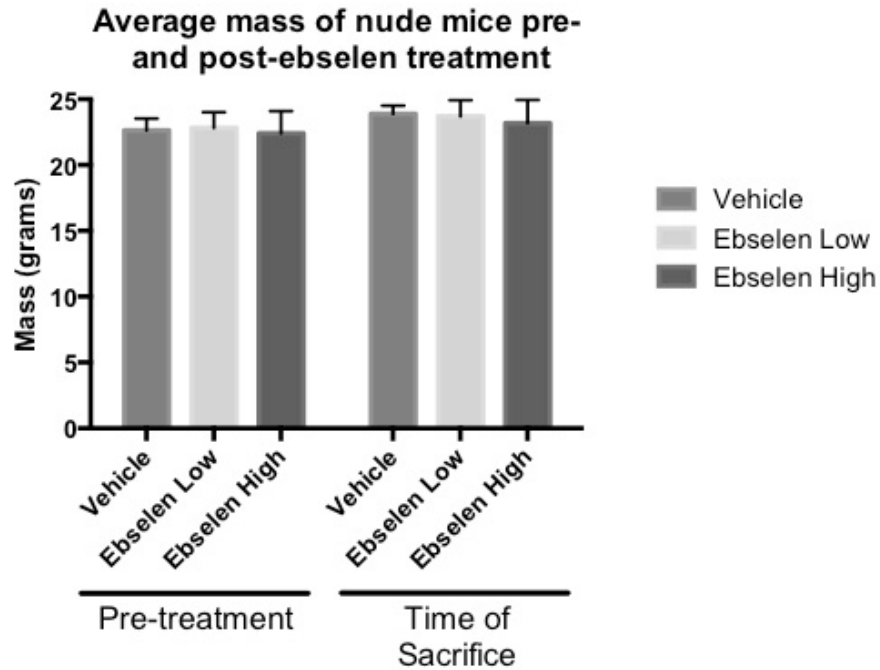
**Figure 9.** Average masses of nude mice pre- and post-ebselen treatment. Nude mice were weighed on a laboratory scale immediately prior to tumor implantation to the nearest 0.1 g. Mice were weighed again at the conclusion of the study, immediately after $CO_2$ asphyxiation. N=5 per group, error bars represent standard deviation.
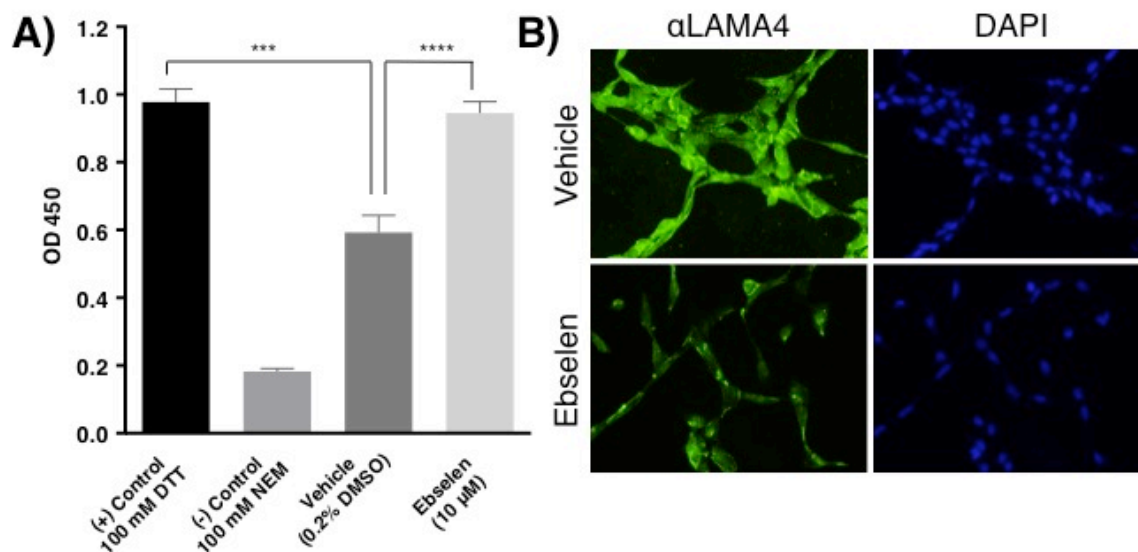
**Figure 10**. Extracellular matrix composition is altered by ebselen treatment. A) Extracellular matrix sulfhydryl quantitation performed on $1 \times 10^4$ MIAPaCa-2 cells exposed to vehicle or 10 μM ebselen for 48 hours. Error bars represent standard deviation. Significance determined by two-tailed T-test, comparing vehicle-treated to SBI-183-treated cells. n = 7 wells averaged per group. B) Immunofluorescence of LAMA4 (left) on 786-O cells treated with either vehicle (top) or 15 μM ebselen (bottom). Images were obtained from identical exposures and were not enhanced. DAPI-stained nuclei are shown at right. Note: vehicle images same as in Figure 23 (both compounds run in same experiment with common control, but separated for the purpose of this document).
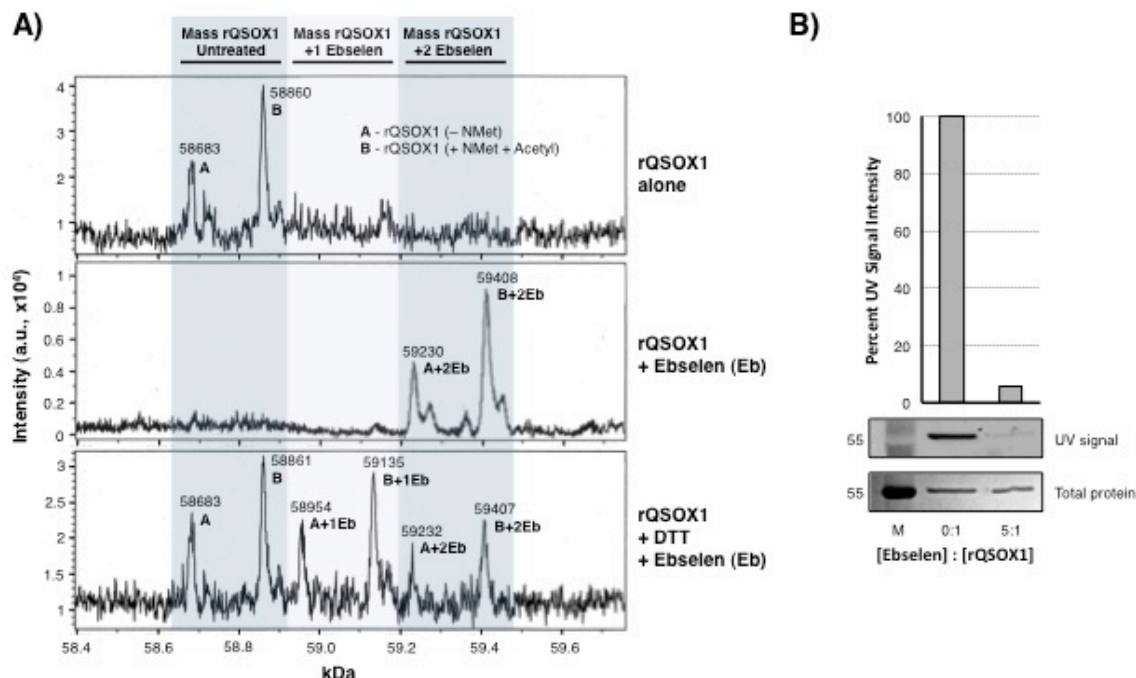
**Figure 11.** Ebselen binds covalently to rQSOX1 at cysteine residues. A) Charge deconvoluted ESI-LC-MS spectra of rQSOX (top spectrum) in the absence of substrate, rQSOX1 treated with 5 μM ebselen (middle spectrum), and rQSOX1 treated with 5 μM ebselen in the presence of DTT substrate (bottom spectrum). The mass of an ebselen adduct is 274.18 Da. The left shaded column indicates the mass range of unmodified rQSOX1. Peak A is the mass of rQSOX1 without the N-terminal methionine and peak B is the mass of rQSOX1 with N-acetyl Met. The middle shaded column represents the mass of rQSOX1 with a single bound ebselen molecule with peaks labeled A+1Eb and B+1Eb. The right shaded column represents the mass of rQSOX1 with two ebselen adducts (A+2Eb and B+2Eb). B) QSOX1 pretreated with ebselen blocks the binding of fluoresceinated maleimide. A 5-fold molar excess of ebselen was added to 5 μg rQSOX1 prior to maleimide addition. UV imaging of SDS-PAGE gels show that maleimide binding to rQSOX1 is blocked by the addition of ebselen.
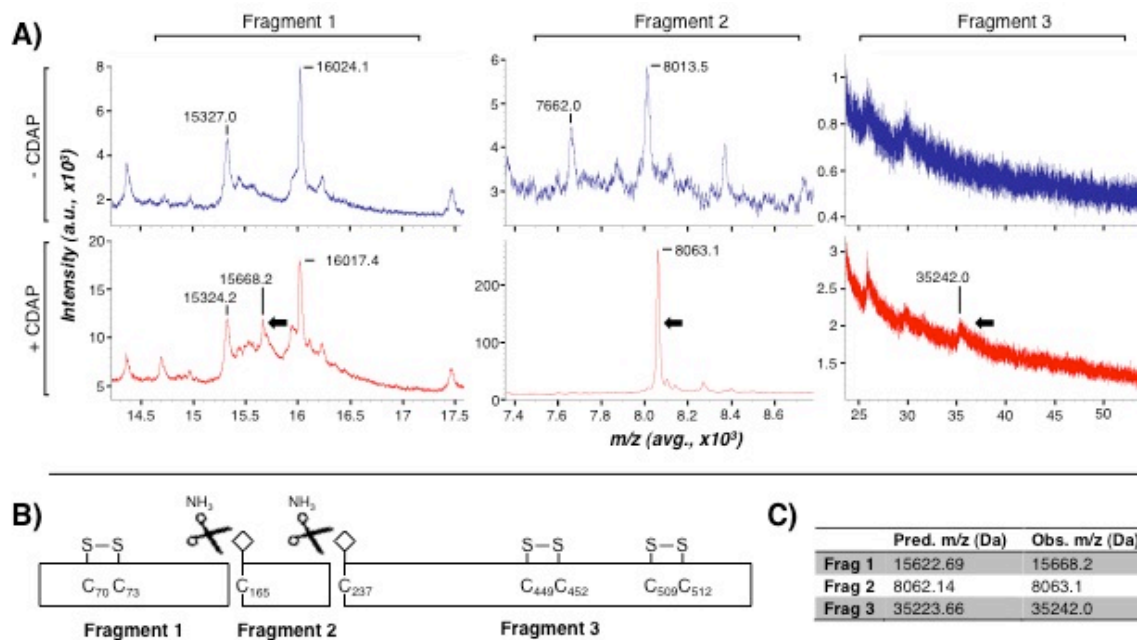
**Figure 12.** Identification of ebselen-binding cysteines in QSOX1. A) Cyanylated rQSOX was cleaved by $NH_3$ treatment and reduced with TCEP. Analysis by MALDI-MS identified two cleavage sites that produced QSOX1 fragments with masses of 15 668 Da (Fragment 1), 8 063.1 Da (Fragment 2), and 35 242 Da (Fragment 3). The top and bottom spectra panels in (blue) show untreated (blue) and CDAP-treated (red) QSOX1 peaks, respectively. Arrows indicate unique peaks appearing in CDAP-treated, but not untreated, rQSOX1 samples. B) Mapped QSOX1 CDAP cleavage fragments. Peak masses correspond to cysteines 165 and 237 in wild-type QSOX1. Cyanyl groups are depicted as white diamonds. Three redox-active C-X-X-C pairs are shown disulfide bonded. The four remaining disulfide-bonded cysteines are not shown. Cleavage of rQSOX1 by ammonia (black scissors) produced the three CDAP fragments observed in (A). C) Predicted and observed average m/z for cleavage at residues C165 and C237. The predicted masses for fragments 2 and 3 include an additional 25 Da from the cyanyl group.

39

**Conclusions:**

In a high throughput screen of the LOPAC[1280] chemical library utilizing recombinant QSOX1, ebselen was identified as an inhibitor of QSOX1 enzyme activity. An *Aspergillus niger* glucose oxidase (GOx) was utilized as a general counter-screen to ensure that inhibition was specific for QSOX1. Although both GOx and QSOX1 contain FAD as a cofactor, the former uses FAD as the initial electron acceptor [58], while FAD serves as terminal electron acceptor in the QSOX1 Erv1 domain. In addition, the sequence and structure of the two proteins are very different [14], sharing only 20% sequence identity. Thus the majority of genuine inhibitors are expected to show strong preference for QSOX1. As seen in supplementary Figure 5, GOx is inhibited by ebselen only at a concentration 4-fold higher than was observed for QSOX1.

Since ebselen reacts with free cysteines and both QSOX1 substrates and its own redox activity are dependent on sulfhydryls, we were initially concerned that the interaction of ebselen with QSOX1 substrates DTT and RNAse A might make ebselen appear to inhibit QSOX1 spuriously through substrate depletion. Concentrations between 150 and 2400-fold molar excesses of substrate thiols over ebselen were used in confirmatory activity assays to guard against this possibility (Figure 6). If the interaction of ebselen with substrate was extensive, even with total exhaustion of ebselen sufficient unreacted substrate would be available for QSOX1 oxidation. These conditions would allow for near-maximum signal to be detected, preventing the identification of compounds with an indiscriminate preference for free cysteines. Additionally, rQSOX1 enzyme was always added last to reactions such that ebselen was present with substrate

before QSOX1 was added. Therefore the excess substrate would deplete available ebselen prior to the addition of active enzyme.

Ebselen treatment of tumor cell lines resulted in significantly decreased invasion in trans-well invasion assays compared to DMSO vehicle-treated cells (Figure 7). These results are consistent with decreased invasion in cells expressing QSOX1-specific shRNAs [35, 38, 45]. Importantly, rescue of invasion in QSOX1-knockdown cells was achieved with the addition of 50 nM exogenous recombinant QSOX1 enzyme (Figure 7A, fifth bar). However, pre-incubation of recombinant enzyme with 10 μM ebselen prior to addition of QSOX1 to tumor cells did not restore invasive activity (Figure 7A, sixth bar), suggesting that ebselen inactivates QSOX1. In fact, tumor cell invasion was further decreased compared to the sh742 knockdowns, underscoring the incomplete suppression of gene expression using a shRNA system. These results indicate that one mechanism by which ebselen decreases tumor cell invasion is via QSOX1 enzymatic inhibition.

The growth modulatory effects of ebselen were investigated in pancreatic and kidney cancer cell lines (Figure 13). Ebselen was a poor inhibitor of growth in kidney cancer cell lines, but did significantly inhibit growth of pancreatic cell line MIAPaCa-2 at 10 μM and 15 μM and BXPC3 at 15 μM. QSOX1 expression was similar for the cell lines tested by western blotting (Figure 14), thus QSOX1 expression alone fails to explain the growth effects observed. Viability determinations showed that ebselen is not cytotoxic to tumor cells (Figure 15), so decreased growth is therefore attributable to reduced proliferation. Ebselen treatment also causes tumor cells to "round up" (data not

41

shown). While anecdotal, this observation is consistent with the morphological changes observed when QSOX1 expression is suppressed by shRNAs [35, 38].

Incubation of 15 μM ebselen with normal lymphocytes and non-malignant fibroblasts does not result in toxicity (~98% viability after 48 hours, data not shown). Additionally, ebselen has an established safety profile and dosing in humans in phase II clinical trials for cerebral infarct [59-61]. Patients in this 1998 clinical trial who received ebselen had no statistical increase in adverse events compared to placebo groups for new cerebral infarction, new hemorrhagic infarction, gastrointestinal bleeding, nausea/vomiting, or respiratory infection. The authors also note that ebselen treatment did not contribute to the death of any patient [61].

Daily oral gavage of ebselen in human pancreatic tumor xenografts resulted in slower tumor growth than vehicle controls. Ebselen appears to suppress invasion and is not directly cytotoxic, but none-the-less affects human pancreatic tumor cell growth *in vivo* as shown in Figure 8. While both low (160 μg/day) and high (640 μg/day) doses of ebselen decreased tumor growth in our xenograft model, differences in tumor volume were not observed between dosages. There may be no additional benefit to treatment with higher doses of ebselen beyond a certain threshold. While the mechanism of decreased tumor cell growth with ebselen treatment is unclear, reduction in the total mass between groups was not the reason for reduced growth, an effect that could be due to decreased appetite or malnourishment associated with ebselen treatment (Figure 9). One explanation for the decrease in tumor growth in mice treated with ebselen is the inhibition of QSOX1 activity in the extracellular matrix. QSOX1 is required for incorporation of

laminin α4 chains in the ECM [45]. Its inhibition may limit the ability of tumor cells to modify the ECM to promote tumor growth. QSOX1 also activates MMP-2 and -9, supporting the role of QSOX1 in forming a pro-tumorigenic microenvironment.

Ebselen is a heterocyclic selenoorganic compound first identified as a glutathione peroxidase mimic and scavenger of organic hydroperoxides [62-64]. The intriguing enzyme-like activity of ebselen forms the basis for its pharmacological effects [65, 66] that include potent antioxidant and anti-inflammatory properties [53, 67]. Ebselen covalently binds to thiols and this has emerged as a mechanism for its activity [68]. Ebselen reacts via reduction of the Se-N bond in the selenazole ring structure, forming a sulfur-selenium bond with target cysteines [69]. Ebselen is shown to inhibit QSOX1 activity through covalent modification of non-redox cysteines C165 and C237 in the extant thioredoxin-2 domain.

Crystal structures of human rQSOX1 show that its cysteines exist as disulfide pairs in the resting enzyme except for cysteines 165 and 237 [20, 70]. How ebselen inhibits QSOX1 through interaction with these residues is unclear because they are not thought to participate in the accepted disulfide relay mechanism. There is no evidence supporting cysteines other than the redox-active C-X-X-C motifs in the Trx1 and Erv domains as contributing to QSOX1 activity [13, 14, 22, 23, 29]. C237 is likely protonated and relatively inert to redox reactions since there are no nearby basic residues to stabilize a thiolate anion [71]. The location of C165 in a predicted disordered region of QSOX1 between the Trx1 and Trx2 domains, however, may allow for interactions with nearby basic resides [70]. A recently described mechanism proposes that the flexible domain

architecture of QSOX1 is critical in allowing Trx1 to come into close contact with Erv to transfer electrons to the C-X-X-C in this domain [20, 21]. Ebselen bound to C165 and C237 may interfere with the conformational change required for the interaction of the Trx1 and Erv domains. Another possibility is that these cysteines modulate the activity of QSOX1; C165 is conserved in QSOX1 among vertebrates but not invertebrates (Figure 16) and may have evolved as a mechanism to regulate QSOX1 function. Further enzymatic and structural studies will address these hypotheses.

Evidence is provided that the inhibition of QSOX1 activity by ebselen leads to significantly decreased invasion of tumor cell lines *in vitro* and reduced tumor growth *in vitro,* and *in vivo*, effects comparable to QSOX1 knockdown. Since metastasis is the cause of most cancer deaths, even partially suppressing invasive processes through QSOX1 inhibition may help prolong survival. This study further establishes QSOX1 as a tractable target for anti-neoplastic drugs. Future studies will identify more potent and specific inhibitors of QSOX1 that may decrease metastasis *in vivo*.
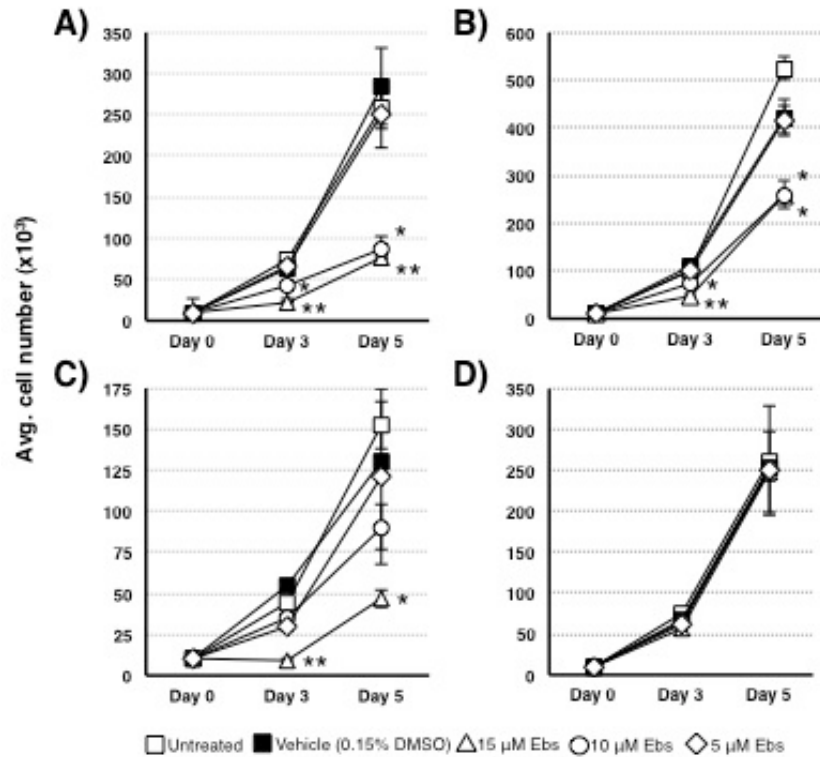
**Figure 13.** Effect of ebselen on growth of tumor cell lines. Cell numbers for tumor cell lines grown in the presence or absence of ebselen or DMSO vehicle are shown. Viable cell numbers were determined manually using Trypan Blue. Each time point was performed in duplicate, and error is represented as SEM. Significance was determined for ebselen-treated cells compared to vehicle-treated cells using paired T-tests. Growth kinetics are shown for A) MIAPaCa-2, B) BXPC3, C) 786-O, and D) UOK117. *p<0.08, **p<0.05. At 5 days incubation, 10 µM ebselen decreased MIAPaCa-2 cell number by 70% compared to vehicle. For BXPC3, day 5 cell numbers were reduced by 38% for both 15 µM and 10 µM ebselen. 786-O and UOK117 were more resistant to ebselen. 15 µM ebselen decreased 786-O growth 79% and 65% at days 3 and 5, respectively. UOK117 growth was unaffected by ebselen treatment at all concentrations tested. It is important to note that the reduced cell numbers observed were not due to decreased viability from ebselen cytotoxicity (Figure 15).

45
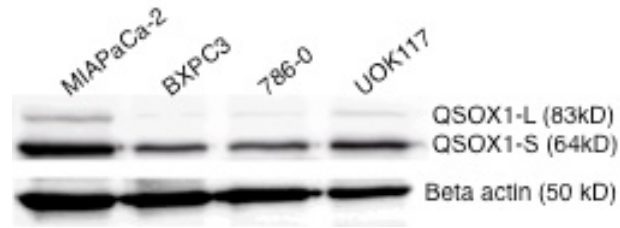
**Figure 14.** Relative QSOX1 expression in pancreatic and renal cancer cell lines. 10 µg total protein loaded in 12% SDS-PAGE gels at 150 V. Proteins resolved and transferred onto PVDF membranes for one hour at 100 V. Membranes blocked for 1 hour with 1% BSA 0.1% TBST at room temperature on shaker. Membranes were incubated with 1:1000 anti-QSOX1 (ProteinTech), or 1:1000 anti-BACTN (Cell Signaling) followed by 1:10,000 goat anti-rabbit HRP for 1 hour at room temperature.
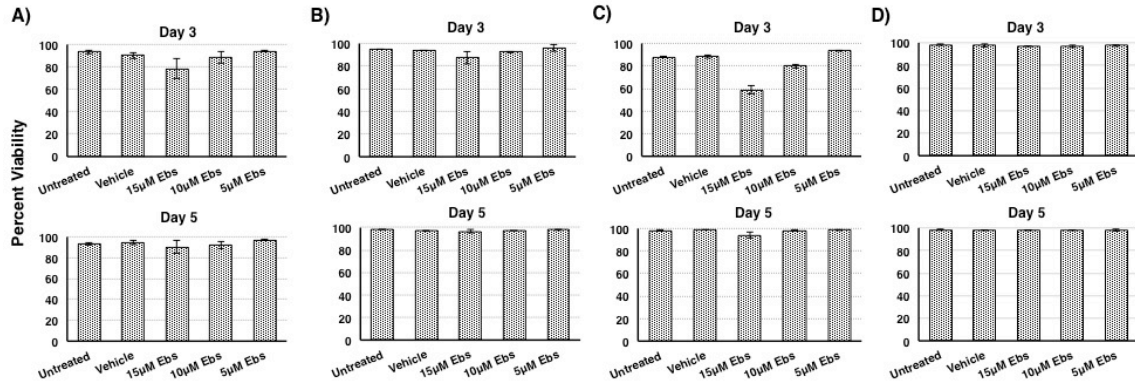
**Figure 15.** Viability of tumor cell lines treated with ebselen. Total viability was determined at days 3 and 5 by Trypan Blue exclusion with 2 counts performed per group. Viability was calculated as [1-(# dead / (# dead + # alive))]*100. Error bars represent SEM. A) MIAPaCa-2, B) BXPC3, C) 786-O, D) UOK117. No appreciable decrease in cell viability was observed up to 15 µM at days 3 and 5, except for 786-O (C) where viability at day 3 was 60%.

```
                    hsQSOX1 C165
H.sapiens        P--PACPPLEPAKLEEIDGFFARN-NEEYLALIFEKGGSYLGREVALDLSQHKGVAVRRV 218
P.troglodytes    P--PACPPLEPAKLEEIDGFFVRN-NKEYLALIFEKGGSYLGREVALDLSQHKGVAVRRV 219
G.gorilla        P--PACPPLEPAKLEEIDGFFARN-NEEYLALIFEKGGSYLGREVALDLSQHKGVAVRRV 218
P.albeii         P--PACPPLEPARLEEIDGFFARN-NEEYLALIFEKGGSYLGREVALDLSQHKGVAVRRV 221
M.mulatta        P--PACPPLEPAKLEEIDGFFARN-KEEYLALIFEKGGSYLGREVALDLSQHKGVVVRRV 218
M.musculus       P--PACPPLEPAKLNDIDGFFTRN-KADYLALVFEREDSYLGREVTLDLSQYHAVAVRRV 221
R.norvegicus     P--PACPPLEPAKLKDINEFFTRS-KAEYLALIFEREDSYLGREVTLDLSQFHAVAVRRV 221
B.taurus         P--PACPPLEPARLEEITGFFARN-NEEYLALIFEKEGSYLGREVTLDLSQHQGIAVRRV 219
G.gallus         P--PACPPLEPASAEEVRSFFHRN-TERYLALIFEQSNSFVGREVALDLLQYENVAVRRV 229
D.rerio          P--PACPPLETASEAEVHHFFPAN-NVKYLALVFENKKSYVGREVTLDLLQYENIAVRRV 227
A.carolinensis   P--PSCPPLEPISAAELHDFFQTN-SVTYLALIFEDENSFLGREVTLDMLQFENIAIRRV 210
X.laevis         P--PACPPLEPISAYEVEQFFITH-QEDYLALIFEEASMYIGRETALDMVQYEGVSVRRV 210
C.capitata       PNYPNLNSLTENEAKTLNKVFTTDSNKKFVILVYEPENSTVGLESILHFHLWSDVQVRRI 235


                    hsQSOX1 C237
H.sapiens        LNTEANVVRKFGVTDFPSCYLLFR-NGSVSRVPVLMESRSFYTAYLQRLSGLTRE----- 272
P.troglodytes    LNTEANVVRKFGVTDFPSCYLLFR-NGSVSRVPVLMESRSFYTAYLQRLSGLTRE----- 273
G.gorilla        LNTEANVVRKFGVTDFPSCYLLFR-NGSVSRVPVLMESRSFYTAYLQRLSGLTRD----- 272
P.albeii         LNTEANVVRKFGVTDFPSCYLLFR-NGSVSRVPVLMESRSFYTAYLQRLSGLTRE----- 275
M.mulatta        LNTEADVVRKFGVTDFPSCYLLFR-NGSVSRVPVLMESRSFYTAYLQRLSGLTRE----- 272
M.musculus       LNTESDLVNKFGVTDFPSCYLLLR-NGSVSRVPVLVESRSFYTSYLRGLPGLTRD----- 275
R.norvegicus     LNSESDVVSKFAVTDFPSCYLLLR-NGSVSRVPVLVESRPFYTSYLRGLPGLTRE----- 275
B.taurus         LNTERDVVNRFGVTNFPSCYLLSR-NGSFSRVPALTESRSFYTTYLRKFSGSTRG----- 273
G.gallus         LSSEEELVEKFGVTTFPSAYLLLR-NGSFSRLPVHAEARSFYTYYLQTLSGVTRG----- 283
D.rerio          LDTETNLVSRFGVTEFPSCYLYDS-SGNITRLKVLKEARTFYSYALQRLPGVVRTG---- 282
A.carolinensis   LQTNEELVKRFNVTSFPSGFLLVN-NGSCSSIPVNADFRPFYRSFLQSLPNVFRGN---- 265
X.laevis         HRDQDDIVNKFQIPSFPALVLLCK-NGSNTIVNMVEDTRSSYTNFLRSLPGVRKG----- 264
C.capitata       N--DINLANTFQIDGGKHKIATVDPQGNVVPYGVTEDTPQAYTATIENLLTAQGFTPRTV 293
```

**Figure 16.** Multi-species alignment of region in the vicinity of C165 and C237 in human QSOX1. Protein sequences for QSOX1 were obtained from UniProt from Homo sapiens (O00391), Pan troglodytes (H2Q0P8), Gorilla gorilla (G3R3B5), Pongo albeii (H2N4I1), Macaca mulatta (F7HHU1), Mus musculus (Q8BND5), Rattus norvegicus (Q6IUU3), Bos Taurus (F1MM32), Gallus gallus (F1NYK2), Danio rerio (B0UXN0), Anolis carolinensis (G1K901), Xenopus laevis (A0JPG9), Ceratitis capitata (W8C0Z9); UniProt ID numbers in parentheses. Seqeuences were aligned using ClustalW2 [72]. Conserved cysteines at human positions C165 and C237 are bolded and colored blue. The cysteine at human position C165 is conserved in sequence from all vertebrate species analyzed, but not in the fruit fly Ceratitis capitata. Human C237 is less conserved, not present in vertabrates G. gallus, A. carolinensis, X. laevis, and the invertebrate C. capitata.

CHAPTER 4

3-METHOXY-N-[4-(1-PYRROLIDINYL)PHENYL]BENZAMIDE (SBI-183)

INHIBITS QSOX1 ENZYMATIC ACTIVITY AND EXERTS BIOLOGICAL

EFFECTS CONSISTENT WITH QSOX1 KNOCKDOWN.

**Overview:**

QSOX1 activity is associated with a proliferative and invasive phenotype in tumor cells, and its enzymatic activity has been shown to be required for many of its biological functions. Previous work has shown that knockdown of QSOX1 leads to decreased tumor growth *in vivo*, and that inhibition of QSOX1 enzymatic activity with a single-chain antibody and a small molecule decreases tumor cell invasion. These results indicate that the QSOX1 inhibition is an attractive area of research from both a basic biological and clinical standpoint. Here we expand on previous work ,and identify ,3-methoxpyrrolidinyl)phenyl]benzamide (SBI-183), as a new small molecule QSOX1 inhibitor. This molecule decreases the growth and invasion of tumor cell lines, as well as the growth of two human renal cell carcinomas (RCC) in nude mouse xenografts, including a highly aggressive sarcomatoid subtype of RCC for which there is no effective treatment. Alterations in the composition of the extracellular matrix were also observed, with an increase in protein thiols and a dramatic reduction in laminin α4 in the ECM. While the inhibitory mechanism of this molecule is not yet known, its biological effects are consistent with QSOX1 knockdown and continue to support the idea that inhibition of QSOX1 has anti-tumorigenic properties *in vitro* and *in vivo*.

**Results:**

*Identification of 3-methoxy-n-[4-(1-pyrrolidinyl)phenyl]benzamide, SBI-0143183 ("SBI-183") as a lead QSOX1 inhibitor.*

A cell-free High Throughput Screening (HTS) assay was employed to identify chemical compounds that inhibited QSOX1 enzymatic activity. HTS was performed by Sanford Burnham Prebys Medical Discovery Institute to screen an in-house library of 50,000 small molecules using a reduced RNAse A substrate of rQSOX1 as described in Chapter 2. Twenty hits were identified in the screen using glucose oxidase counterscreen as a control in a primary screen and a confirmatory assay (see Appendix A for $IC_{50}$ data on these 20 compounds). A secondary confirmatory assay was performed using an HVA-based activity assay using a DTT substrate (Figure 17). In the HVA assay, SBI-0143183 (SBI-183) suppressed the activity of QSOX1 by 64.8% (Figure 17A) compared to a DMSO vehicle. As an additional control, it was determined that the reduced enzymatic activity observed was not due to the scavenging of $H_2O_2$ by SBI-183, a common issue in small molecule screens that quantify the production of $H_2O_2$ (Figure 17B). The structure of SBI-183 is shown in Figure 17C.

The 20 hit compounds were also screened for their growth inhibitory activity against tumor cell lines (Figure 18). Renal cancer cell line 786-O (Figure 18A), or pancreatic cancer cell line MIAPaCa-2 (Figure 18B) were exposed to 20 μM, 10 μM, or 5 μM SBI-183 for 72 hours. Cells were analyzed by MTT and are represented as percent vehicle signal. SBI-0143183, SBI-0132719, SBI-0099708, and SBI-0132719 had the largest growth inhibitory effect on 786-O cells, while SBI-0143343, SBI-0143183, SBI-

0137402, SBI-0132719, SBI-0035734, SBI-0099708, and SBI-0129659 were most active

against MIAPaCa-2. Since SBI-183 showed both inhibition of rQSOX1 enzymatic

activity and suppression of tumor cell growth in both 786-O and UOK117, it was selected

as a lead compound for further analysis.

*Dose response curves for SBI-183 reveal a large therapeutic window*.

The IC$_{50}$s for tumor cells and healthy donor lymphocytes were determined by

MTT assay (Figure 19). $5x10^3$/well 786-O, UOK117, and A498 (Figure 19A) or $1x10^5$

peripheral blood mononuclear cells (resting or stimulated with 10 μg/ml PHA (Figure

19B), were treated with 2-fold dilutions of SBI-183 between 80 μM and 160 nM (in

triplicate), and incubated for 48 hours and then analyzed. Potent inhibition of growth was

observed for 786-O, UOK117, and A498, with IC50s of 1.25 μM, 2.86 μM, and 3.37 μM,

respectively. PBMC were strongly resistant to SBI-183, with an IC50 of 81.25 μM for

resting PBMC and 33.4 μM for PHA-stimulated PBMC. Based on these results, a

conservative therapeutic window of 9.9-fold was estimated (based on the fold difference

between PHA-stimulated PBMC and A498 cells).

*SBI-183 potently inhibits tumor cell growth in vitro*.

QSOX1 knockdown decreases tumor cell growth *in vitro* [35, 38]; it was

hypothesized that SBI-183-treatment of tumor cell lines would result in reduced tumor

cell growth over time. Tumor cell lines were treated for a period of 5 days with SBI-183

and assayed cells for growth (Figure 20). $1.25x10^3$ 786-O and UOK117 cells per well

were added to plates and incubated overnight in 96-well plates. 5 µM, 2.5 µM, 1.25 µM, 625 nM SBI-183, or 0.05% DMSO vehicle was added in triplicate and cells were incubated. Plates were analyzed at day 0 (baseline, before compound addition), day 3, and day 5. For 786-O (Figure 20A), 625 nM and 1.25 µM had modest, but significantly reduced growth by day 5, with 12% reduced growth each. 2.5 µM SBI-183 reduced growth by 35% at day 5, and 5 µM decreased growth 89.8% at day 5. UOK117 was more sensitive to the SBI-183, and cytotoxicity was observed at 2.5 µM and 5 µM (Figure 20B). 1.25 µM SBI-183 reduced the growth of UOK117 by 91%, whereas 625 nM showed a 20% reduction at day 5.

*SBI-183 suppresses tumor cell invasion in vitro.*

QSOX1 knockdown decreases the invasive capacity of pancreatic and breast tumor cell lines. SBI-183 was tested for its ability to suppress tumor cell invasion in an *in vitro* trans-well migration assay (Figure 21). $2.5 \times 10^4$ 786-O and UOK117 were plated per well in trans-well inserts in starvation media containing 10 µM and 5 µM SBI-183, or 0.1% DMSO vehicle. Inserts were incubated in wells containing complete media for a period of 20 hours, after which the number of invading cells were quantified. Compared to vehicle treated cells, 10 µM and 5 µM SBI-183 treatment resulted in 70% and 54% reduction in 786-O invasion, respectively (Figure 21A). In UOK117 cells (Figure 21B), invasion was reduced by 70% with 5 µM SBI-183, and 87% with 10 µM. These results show that SBI-183 has anti-invasive properties *in vitro*, consistent with both QSOX1

knockdown as well as enzymatic inhibition by ebselen as reported previously [35, 38, 48].

*Daily oral gavage of SBI-183 retards the growth of 786-O and UOK117 xenograft tumors in a nude mouse model.*

Nude mice injected with MIAPaCa-2 tumors were treated daily with the QSOX1 inhibitor ebselen show reduced tumor growth compared to untreated or vehicle-treated controls [48]. SBI-183 was tested determine whether it exhibited similar activity as ebselen and shQSOX1-expressing tumors in suppression of tumor growth [48] using nude mouse xenografts of renal cancer cell lines 786-O and UOK117 (Figure 22). As described in Chapter 2, $1x10^6$ tumor cells were subcutaneously injected into the right hind flank and tumors were established for 1 week prior to initiation of daily oral gavage of 400 μg/mouse/day SBI-183 dissolved in 100% DMSO. Control mice receiving no treatment and those receiving vehicle alone were also tested. Regular length, width, and depth measurements were obtained using Vernier calipers at the intervals indicated in Figure 22. SBI-183-treated 786-O xenografts had average tumor volumes that were 74.9% and 72.1% smaller than vehicle treated mice (Figure 22A). Similarly, mice treated with SBI-183 had significantly reduced UOK117 tumor volumes compared to vehicle, 64.8% smaller on day 17, and 59.1% on day 19 (Figure 22B). There was no statistical difference in the tumor volumes of vehicle and untreated mice for either cell line. These results indicate that SBI-183 inhibits the growth of a human sarcomatoid renal cell carcinoma in an *in vivo* xenograft model.

*SBI-183 treatment increases sulfhydryl concentrations and reduces the deposition of laminin in the ECM of tumor cell lines.*

Sulfhydryl groups on cysteines in reduced proteins may be substrates for QSOX1. While few specific substrates are known, it was shown recently that QSOX1 knockdown increases ECM thiols generally, and leads to defects in the incorporation of laminin α4 into the ECM [45]. We sought to determine if QSOX1 inhibition by SBI-183 led to a similar phenotype (Figure 23). $1 \times 10^4$ MIAPaCa-2 cells per well were plated in a 96-well plate and grew them for 48 hours in the presence of 10 μM SBI-183. The cell monolayer was de-roofed, and sulfhydryls in the ECM were quantified using a maleimide-PEG$_2$-biotin probe (Figure 23A). Before labeling, control wells were treated with 100 mM DTT to expose a theoretical maximum of sulfhydryls through reduction of disulfide bonds, or with 100 mM N-ethyl maleimide for a control to quench exposed sulfhydryls. The binding of maleimide-PEG$_2$-biotin to ECM sulfhydryls using streptavidin-HRP and developed wells using a TMB substrate. Compared to DTT-treated cells, vehicle-treated cells showed a 40% reduction in ECM sulfhydryls (p=0.0005). The sulfhydryl concentration in SBI-183-treated cell ECM was increased 61.5% compared to vehicle (p<0.0001), suggesting that SBI-183 inhibition of QSOX1 leads to an increase in ECM sulfhydryls, consistent with a QSOX1 inhibitor.

786-O cells plated on poly-L lysine-coated coverslips were incubated for 48 hours with SBI-183 or DMSO vehicle, fixed, permeabilized and then stained with LAMA4 polyclonal antibody. Images were captured showing the intensity of laminin staining in the ECM (Figure 23B). Significantly reduced LAMA4 was observed in SBI-183-treated

cells, suggesting that QSOX1 inhibition by SBI-183 results in observable defects in ECM composition normally associated with QSOX1 activity.
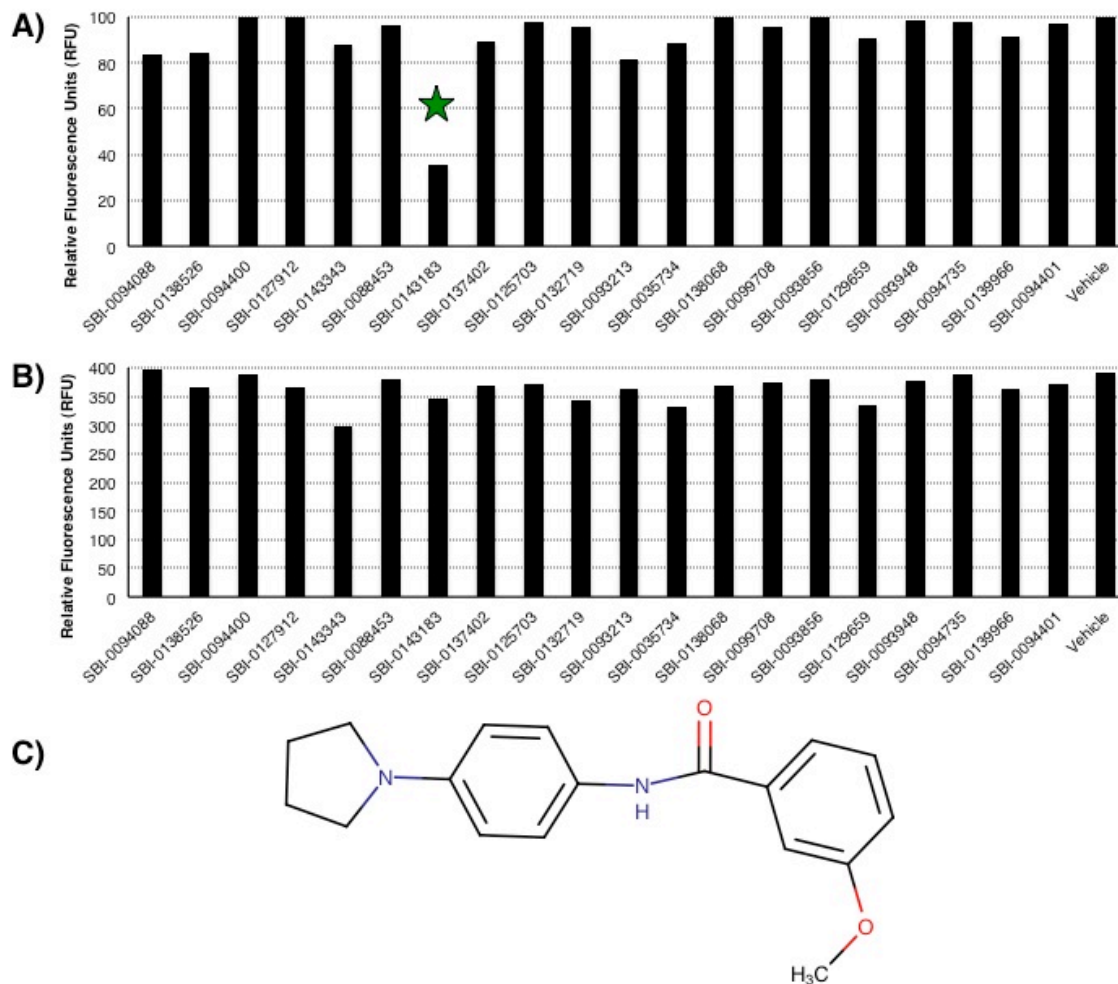
**Figure 17**. HVA-based QSOX1 activity assay confirms SBI-183 as a QSOX1 inhibitor. A) The activity of rQSOX1 exposed to 10 μM each of 20 hit compounds from an initial high throughput screen was determined compared to 0.1% DMSO vehicle. Shown is the total fluorescence after 10 minutes, represented as relative fluorescence units (RFU). Green star indicates rQSOX1 activity with exposure to SBI-183. B) Assays performed in the absence of rQSOX1 were supplemented with 5 μM $H_2O_2$ to ensure that scavenging of $H_2O_2$ or inhibition of HRP did not yield false positives. C) Structure of SBI-183.
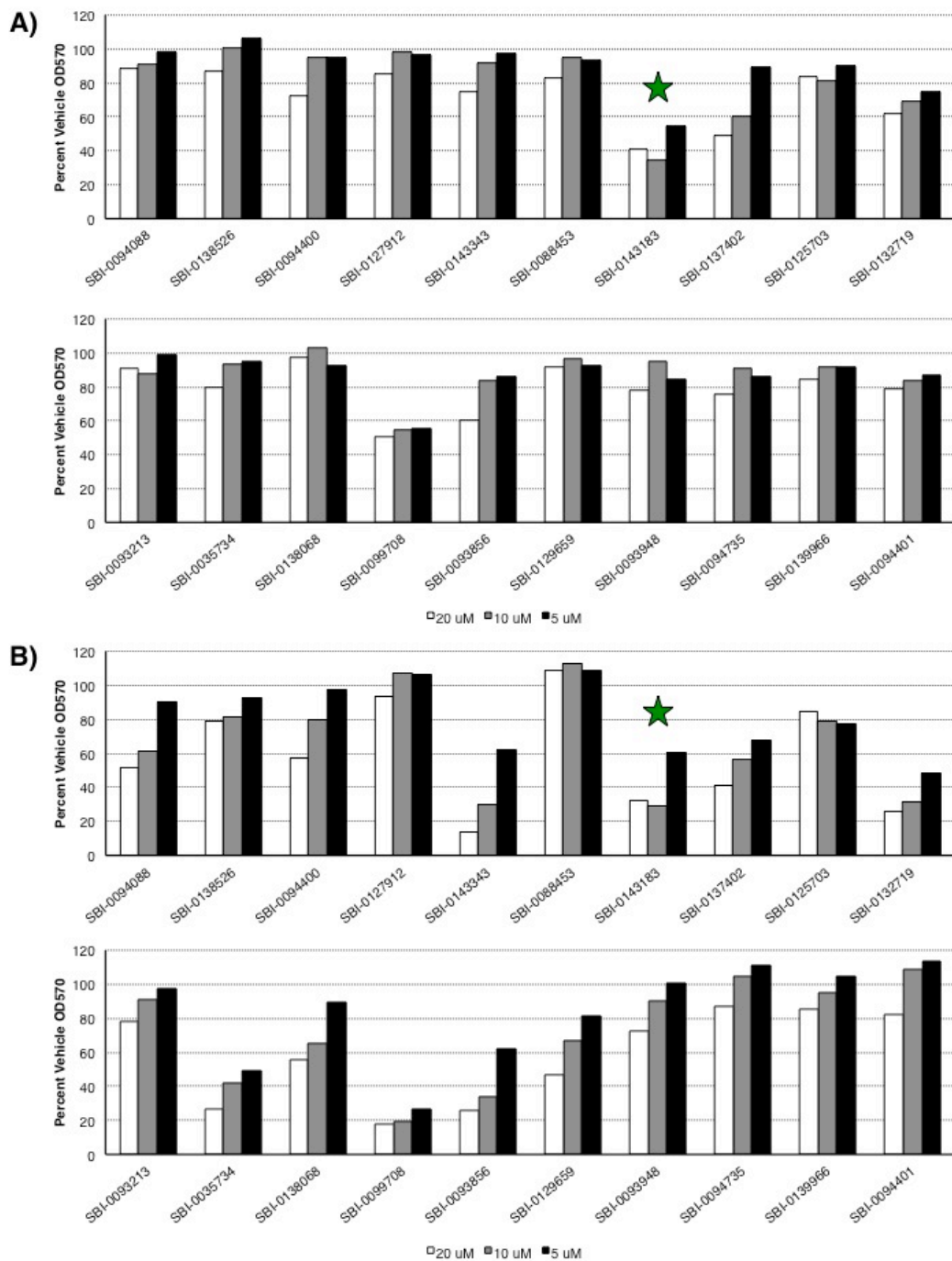
**Figure 18**. Variable growth of tumor cell lines exposed to 20 hit compounds from high throughput screen for inhibitors to QSOX1 confirms anti-proliferative effect of SBI-183 on renal cancer cell line 786-O (A), and pancreatic tumor cell line MIAPaCa-2 (B). Cells were exposed to compounds in complete media after overnight adherence and incubated for 72 hours followed by MTT analysis. Green star indicates cells treated with SBI-183.
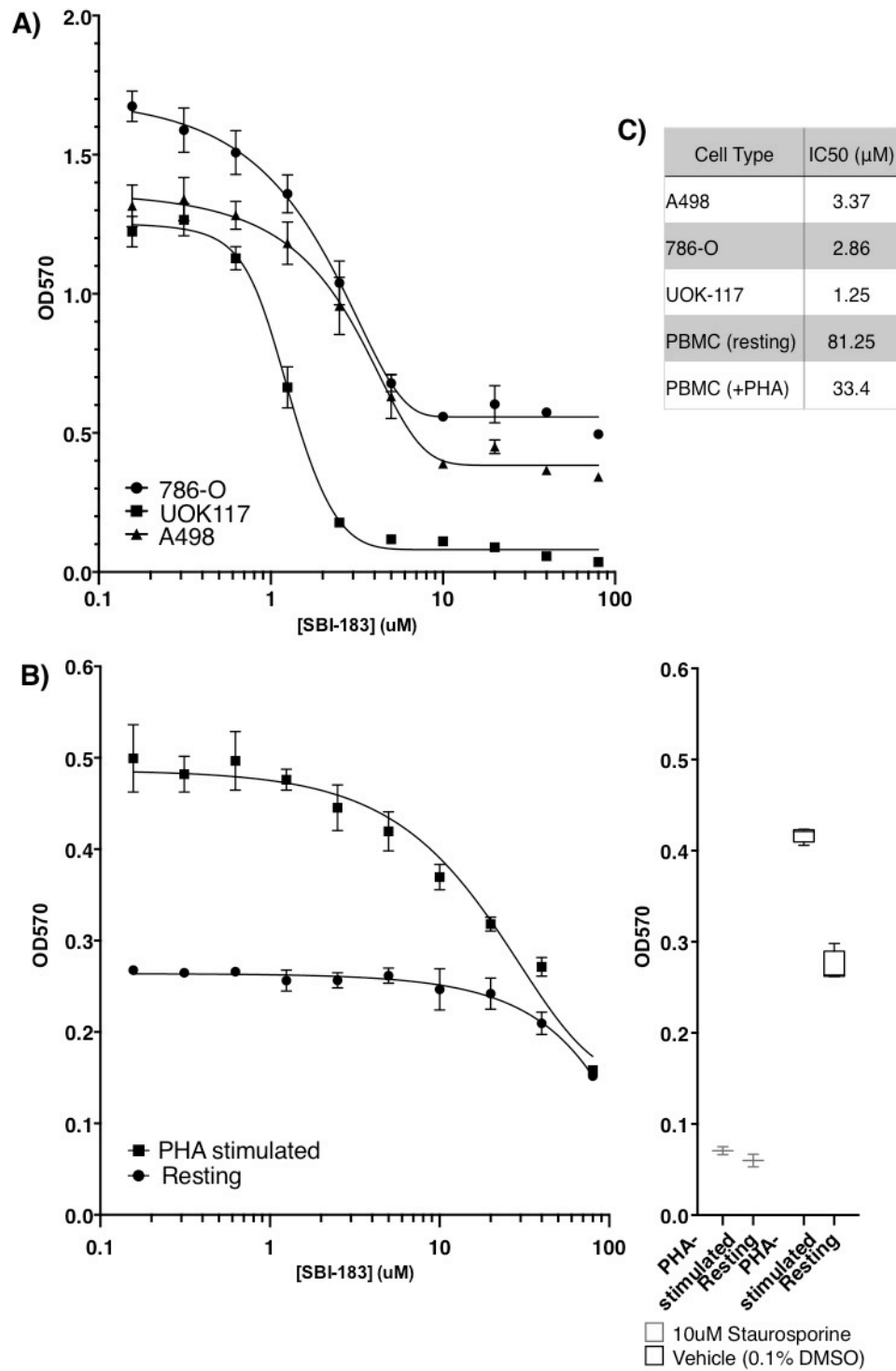
**Figure 19.** SBI-183 dose responses for tumor cell lines and healthy donor lymphocytes. A) Renal cancer cell lines 786-O, UOK-117, and A498 or B) Primary donor lymphocytes (either resting or stimulated with 10 μg/ml PHA) were exposed to compound for 48 hours and analyzed by MTT. For lymphocytes, the bottom of the curve

was determined from incubation of cells with 10 µM Staurosporine (B, right). Error bars represent standard deviation. C) IC50 values for SBI-183. IC50s for PBMC were determined using Staurosporine control.
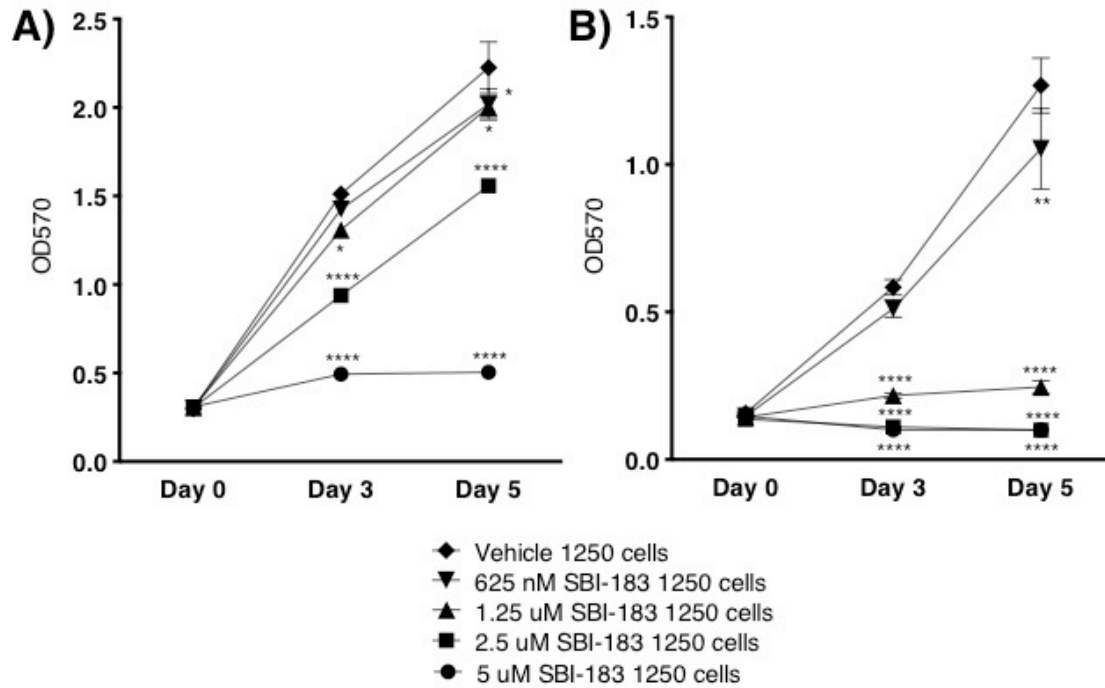
**Figure 20.** SBI-183 decreases the rate of tumor cell growth. 1,250 cells per well of A) 786-O, or B) UOK117 were plated in triplicate in 96-well plates and adhered overnight. At the time of compound addition, an MTT assay was performed to determine the baseline ("Day 0") signal for each condition. Media containing SBI-183 at the indicated concentrations (or vehicle, 0.05% DMSO) was then added. Plates were analyzed by MTT at days 3 and 5 after compound addition. Error represents standard deviation. Significance was determined by 2-way ANOVA, * $p<0.05$, **$p<0.01$, ****$p<0.0001$.
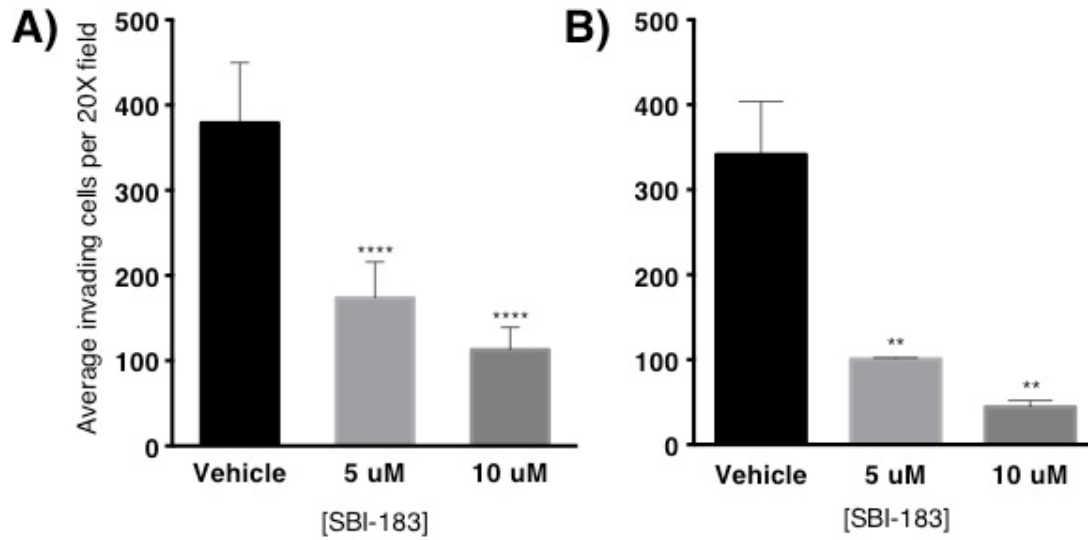
**Figure 21.** SBI-183 decreases invasion of renal cancer cell lines in a transwell migration assay. $2.5 \times 10^4$ A) 786-O or B) UOK117 cells were adhered for 2 hours in serum-free media in transwell inserts and then exposed to 5 μM or 10 μM SBI-183 for 20 hours. Invasion was quantified as the average number of invaded cells per 20X field, n=3 unique fields counted per group. Significance was determined by two-tailed T-test, comparing SBI-treated cells to vehicle. Error bars represent standard error of the mean, **p<0.01, ****p<0.0001.
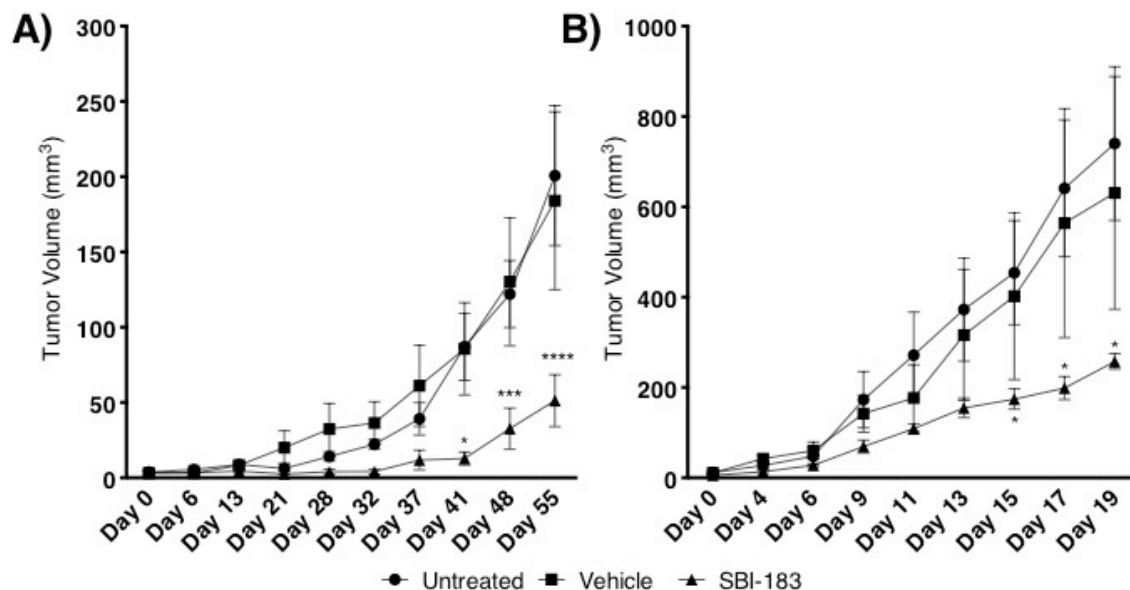
**Figure 22**. Growth kinetics of xenografted tumors in nude mice treated with SBI-183. $1x10^6$ A) 786-O and B) UOK117 were subcutaneously injected into nude mice and tumors were established before initiation of daily oral gavage of 400 µg/day SBI-183 or 100% DMSO vehicle. Real-time tumor measurements were taken at regular intervals, measuring length, width, and depth. Untreated mice are represented as closed circles, vehicle treated mice as closed squares, and SBI-treated mice as closed triangles. For 786-O, n=5 mice per group except SBI-183 (n=4). For UOK117, n=5 mice per group, except vehicle (n = 4). Error bars represent standard error of the mean. Significance was determined by two-way ANOVA. *$p<0.05$, ***$p<0.001$, ****$p<0.0001$.
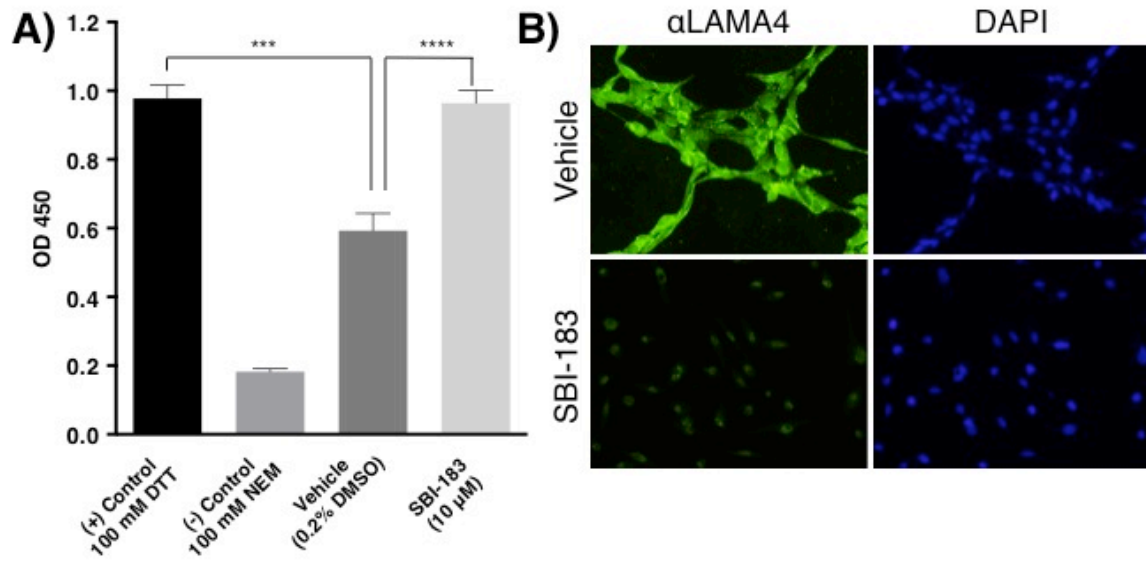
**Figure 23**. Extracellular matrix modulation by SBI-183. A) Extracellular matrix sulfhydryl quantitation performed on $1x10^4$ MIAPaCa-2 cells exposed to vehicle or 10 µM SBI-183 for 48 hours. Error bars represent standard deviation. Significance determined by two-tailed T-test, comparing vehicle-treated to SBI-183-treated cells. n=7 wells averaged per group. B) Immunofluorescence of LAMA4 (left) on 786-O cells treated with either vehicle (top) or 15 µM SBI-183 (bottom). Images were obtained from identical exposures and were not enhanced. DAPI-stained nuclei are shown at right.

**Conclusions:**

In collaboration with Sanford Burnham Prebys Medical Discovery Institute, rQSOX1 was screened against an in-house 50,000 compound library in a high-throughput enzymatic activity assay modified for luminescent output from an assay developed by Colin Thorpe's group [25]. Twenty compounds were identified as potential QSOX1 inhibitors (Appendix A). These compounds were obtained and re-tested at a concentration of 10 μM using an HVA-based assay (Figure 17). In this assay, most compounds showed modest inhibition of QSOX1 (Figure 17A), but no apparent scavenging of hydrogen peroxide or HRP inhibition (Figure 17B). The differences observed between the primary and confirmatory assays may reflect a difference in inhibitory capacity with respect to QSOX1 substrate preference; Sanford Burnham Prebys used a reduced RNAse A substrate whereas the confirmatory assay was performed using a model QSOX1 substrate, DTT. In future screens and structural optimization studies it may be therefore useful to utilize a validated QSOX1 substrate from the ECM to obtain inhibition data informative of QSOX1 activity in a more realistic context. An additional possibility for this discrepancy could result from inherent differences in measuring the activity of potential inhibitors using these enzymatic assays. For example, in the initial small molecule screen for ebselen [48], ROS Glo and HyPerBlu assays yielded different IC50 values (1.0 versus 5.4 μM, respectively), underscoring the need for confirmatory assays to lend confidence in moving forward with potential lead compounds; SBI-183 was active in multiple QSOX1 activity assays. The use of biological screens is also critical, as determining a biological phenotype consistent with

64

inhibition of the target enzyme is a powerful and necessary confirmation of target specificity. SBI-183, for example, showed growth inhibitory effects (Figure 17B) consistent with QSOX1 knockdown [35, 38]. While other compounds from the screen also showed growth inhibition, further enzymatic studies should be performed before proceeding with their full characterization, such as oxygen consumption assays or biological target modulation, to add confidence in their potential utility.

The growth inhibitory effect of SBI-183 was determined for several kidney cancer cell lines (Figure 19A): 786-O, UOK117, and A498, as well as a normal control cell type: peripheral blood mononuclear cells from a healthy donor (Figure 19B). A potent inhibitory effect of SBI-183 was observed in the tumor cell lines, with IC50's of 2.86 μM, 1.25 μM, and 3.37 μM for 786-O, UOK117, and A498, respectively. Remarkably, the IC50 for PBMC's were 81.25 μM for resting PBMC and 33.4 μM for PHA-stimulated cells (Figure 19C). The large difference between these potencies suggest a reasonable therapeutic window, conservatively estimated at 9.9-fold when comparing the IC50's of A498 and PHA-stimulated lymphocytes. It is of note that resting lymphocytes do not express QSOX1 and PHA-stimulated lymphocytes express extremely low levels of QSOX1-S [73], suggesting that the difference in relative potency of SBI-183 could be due to the high expression of QSOX1 in tumor cells.

Building upon the relative growth inhibitory effect on tumor cells after acute SBI-183 exposure, the growth kinetics of 786-O and UOK117 were studied with extended SBI-183 treatment. Reduced growth rates in cells were observed, commensurate with their IC50 values. For 786-O, significantly reduced proliferation was observed with all

65

concentrations tested: 12% for 625 nM and 1.25 µM, 35% with 2.5 µM, and 89.8% with

5 µM. Cytotoxicity was observed in UOK117 at higher concentrations, with cell death

observed with 5 µM and 2.5 µM. 1.25 µM SBI-183 reduced UOK117 proliferation by

91%, and 625 nM 20%. Both cell lines express similar levels of QSOX1 (Figure 14), so

the differences observed in growth may be more complicated than a QSOX1 mechanism

alone. Perhaps the cell lines differ in their expression of the targets of QSOX1 in the

ECM. Ebselen, a documented inhibitor for QSOX, also showed variable growth effects

presumably due to the fact that ebselen inhibits other proteins, and complex pathways

interact to regulate cell growth and progression through the cell cycle [74]. Of note is the

fact that the specific mechanism of how QSOX1 reduces tumor cell growth is

uncharacterized.

Promotion of an invasive and migratory phenotype is a well-documented and

compelling phenotype associated with QSOX1 activity having important implications in

tumorigenesis [22, 35, 38, 48, 75]. It was shown previously that the selenium-containing

small molecule ebselen exhibited potent anti-invasive activity with a QSOX1-dependent

mechanism (Figure 7)[48]. The activity of SBI-183 was similarly tested in a trans-well

migration assay using the renal cancer cell lines 786-O and UOK117 (Figure 21). A

significant reduction in invasion of these cell lines was observed with SBI-183 treatment,

70% and 54% for 786-O and 87% and 70% for UOK117 with 10 µM or 5 µM,

respectively. These results emphasize the potential utility of small molecule inhibitors of

QSOX1 in mediating anti-tumorigenic properties associated with its enzymatic activity.

Our *in vivo* renal cancer xenografts showed a statistically significant reduction in tumor growth for SBI-183-treated mice harboring both 786-O and UOK117 tumors. UOK117 vehicle-treated and untreated tumors grew very rapidly, reflecting of their sarcomatoid renal cell carcinoma lineage [76, 77], showing an increase in tumor volume of 40.3% in only 2 days for vehicle-treated mice, whereas tumor volume in SBI-183-treated mice increased just 14% in the same period (Figure 22B); the final average tumor volumes of SBI-183-treated mice was just 40.8% of vehicle-treated. Similarly for 786-O tumor-bearing mice, in a 4 day period vehicle-treated mice had an average tumor volume increase of 40% in 4 days, while the average tumor volume increased just 9.4% at the same time for SBI-183-treated mice, with a final average tumor volume just 27.9% of vehicle-treated tumors. In both cases, however, tumor growth was not totally inhibited and tumors did continue to grow, albeit at a reduced rate. This was also observed for both ebselen treatment of nude mice bearing MIAPaCa-2 tumors as well as those with reduced QSOX1 expression from shRNA-mediated knockdown.

The extracellular matrix is an important regulator of normal cellular processes, providing the structural characteristics that support specific cell lineages [42]. The ECM also contains a broad signaling capacity that regulates cellular function and fate, and these properties are intrinsic to the local composition of cellular ECM [43]. Tumor cells modulate the local tumor microenvironment to promote dedifferentiation, growth, invasion, and immune evasion [44]. For example, in renal cell carcinomas and other cancers, laminins that contain α4 chains normally expressed by mesenchymal tissues to promote migration of inflammatory hematopoetic cells (like laminin-411 and laminin-

421). Laminins are upregulated in tumors and have de-adhesive properties that promote tumor cell invasion [47]. In fact, downregulation of α4 laminins leads to decreased invasion of glioma cells [46]. Laminin α4 is an established QSOX1 substrate, and decreased expression of QSOX1 leads to defects in its deposition in the ECM of tumor cells [45]. SBI-183 treatment of 786-O renal cancer cells resulted in a marked defect in laminin α4 observed by immunofluorescence staining (Figure 23B), supporting the anti-invasive properties of the compound through QSOX1 inhibition.

QSOX1 knockdown also increases cysteine thiols in the ECM compared to control cells [45], representing potential QSOX1 substrates that are not currently known. Treatment of MIAPaCa-2 cells with SBI-183 markedly increased the incidence of sulfhydryls in the MIAPaCa-2 ECM (Figure 23A), suggesting that it has potential utility in discovering new QSOX1 substrates leading to a better understanding of QSOX1 biology and its role in tumorigenic processes.

The precise mechanism by which SBI-183 inhibits QSOX1 is not known, but future studies aim to address this important question. Mass spectrometric analysis of rQSOX1 did not result in the detection of stable adducts (Figure 24) like in the case of ebselen [48]. rQSOX1 alone was detected at the expected molecular weight of 58.8 kDa (Figure 24A); rQSOX1 exposed to SBI-183 did not result in an increase in the molecular weight of rQSOX1 (Figure 24B), indicating that the compound does inhibit QSOX1 through covalent interaction.
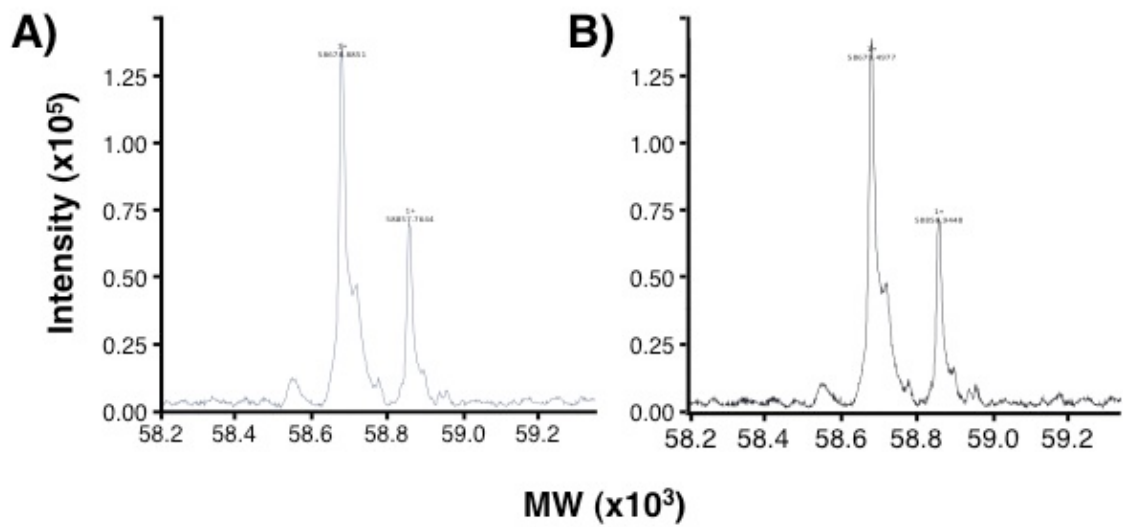
**Figure 24.** Mass spectrum of 12 pmol recombinant QSOX1 A) alone, or B) exposed to 5 μM SBI-183 and analyzed by LC-MS.

CHAPTER 5

DISCUSSION AND CONCLUSIONS

QSOX1 is an emerging target in tumor biology that promotes tumor cell growth, invasion, and the alteration of extracellular matrix composition [22, 35, 37-39, 45]. Extracellular QSOX1 acts directly in the ECM to enhance tumorigenic processes as a consequence of its enzymatic activity. Deposition of a pro-invasive laminin subunit is inhibited by the suppression of QSOX1 in conjunction with an increase in ECM sulfhydryls [45]. The activity of the proteolytic enzymes like MMPs -2 and -9 are increased with elevated expression of QSOX1, suggesting a possible mechanism for the invasive properties exhibited by tumor cells expressing QSOX1 [22, 35, 38, 48]. While the *in vitro* effects of QSOX1 inhibitors have shown early promise in providing target specificity and demonstrate functional effects consistent with a QSOX1 knockdown phenotype, further investigation of these inhibitors including their pharmacokinetic and pharmacodynamic properties are needed. The optimization of inhibitor binding through rational model-based structural augmentation may, additionally, lead to greater specificity and increased biological potency [78, 79]. Such studies in conjunction with pre-clinical models will help to determination of the potential therapeutic efficacy of these compounds. Inhibition of QSOX1 in the clinic has the potential to decrease growth and invasion of tumors, possibly containing primary growth and increasing survival.

Here we establish that QSOX1 promotes tumor growth *in vivo*, strengthening the connection between elevated QSOX1 expression and tumor aggression [31, 38, 39]. MIAPaCa-2 tumor xenografts with stable QSOX1 knockdowns grew in nude mice at

significantly reduced rates compared to controls (Figure 4). These data support other studies demonstrating a pro-tumorigenic role for QSOX1 [22, 31, 33, 35, 37-39, 45]. The enzymatic activity of QSOX1 is essential for its roles in invasion and regulation of extracellular matrix composition [38, 45]. Active, but not inactive, recombinant QSOX1 rescues an invasive phenotype in tumor cells with reduced QSOX1 expression [38]. Also, an inhibitory single-chain antibody developed by the Fass group blocks QSOX1 activity and reduces the invasion of tumor cells across a fibroblast monolayer [45]; these results support the idea that directly targeting QSOX1 enzyme activity has anti-invasive properties. Thus, small molecule inhibition of QSOX1 may have therapeutic efficacy or reveal novel pathways in QSOX1 biology.

An enzymatic activity assay utilizing recombinant QSOX1 and a reduced protein substrate was used by Sanford Burnham Prebys Medical Discovery Institute to screen two small molecule libraries, the LOPAC[1280] and an in-house 50,000 compound library. Two small molecules, 2-phenyl-1, 2-benzisoselenazol-3-one (ebselen), and 3-methoxy-n-[4-(1-pyrrolidinyl)phenyl]benzamide, were identified as lead compounds (Figures 5 and 17) and analyzed further to determine their biological effects in tumor cells with elevated QSOX1 levels and for mechanistic determination of their inhibitory properties against the recombinant enzyme. Ebselen, a small heterocyclic selenium-containing molecule [80], potently inhibits QSOX1 decreasing tumor cell growth *in vitro* (Figure 13) and *in vivo* (Figure 8), similar to QSOX1 knockdown [48]. Invasion of pancreatic tumor cell lines MIAPaCa-2 and BXPC3, and renal cancer cell lines 786-O and UOK117, were decreased upon ebselen treatment (Figure 7). Importantly, ebselen reduces invasion specifically

71

through QSOX1 inhibition (Figure 7A, far right), overcoming the rescue phenotype associated with the exogenous addition of active enzyme (Figure 7A, second from right). This result is significant and agrees with other reports regarding the contribution of QSOX1 to invasion [22, 35, 38], an event in tumorigenesis intrinsically linked to modification of the tumor microenvironment that often precedes metastatic spread [81, 82]. However, it has been reported that the genetic backgrounds of metastatic lesions are, in some cases, very different than that of the primary lesion [83-85]. It would therefore interesting to investigate the expression of QSOX1 by primary tumor sub-populations and metastatic lesions to determine if there is enrichment of QSOX1-expressing cells in a highly aggressive context; modification of extracellular matrix composition at pre-metastatic niche to promote metastasis, for example, may suggest a role for QSOX1 in this process [86-88]. Additionally, the contribution of QSOX1 activity in the tumor microenvironment as it relates to the behavior of the complex stromal milieu, including cancer-associated fibroblasts and cancer stem cells, is of interest given that their tumor-promoting activity are, in part, enhanced by remodeling of the extracellular matrix [89-92]. This also underscores the critical importance of defining the catalog of QSOX1 substrates, which will provide invaluable clues to its role in tissue remodeling promoting tumor growth and invasion.

Treatment of nude mice with ebselen resulted in decreased tumor growth over a 28-day period (Figure 4), suggestive that the enzymatic activity of QSOX1 may also be responsible for its *in vivo* growth inhibitory properties. Previous studies have not investigated the mechanism underlying decreased growth, but it is also important to note

that there may not be a direct effect by QSOX1; rather, involvement of an unknown

QSOX1 substrate may enhance tumor growth. Ebselen itself is known to inhibit a variety

of other enzymes [68, 69] and, given the large number of overlapping pathways that

stimulate proliferation, the use of a promiscuous inhibitor to probe the exact mechanism

of growth modulatory effects would be better performed in a controlled knockout

scenario or with the use of an exquisitely specific inhibitor. Complicating results obtained

for tumor cell growth *in vitro* was the observation that ebselen inhibited many, but not

all, of the tumor cell lines investigated (Figure 13), even though the relative expression of

QSOX1 was similar (Figure 14). UOK117, for example, showed robust QSOX1 levels

but was unaffected by ebselen with respect to growth (Figure 13D) – it was, on the other

hand, very responsive to the anti-invasion effects of ebselen in accordance with the

demonstration of the QSOX1-dependent interaction of ebselen in suppressing this

hallmark phenotype. However, the substrates of QSOX1 are poorly defined, and there are

no reports of QSOX1 directly influencing the expression of downstream factors which

may contribute to tumorigenic processes. So, while QSOX1 levels may be similar among

tumor cell lines of different histological types, this does suggest that the abundance of

different substrates influencing processes like growth and invasion are similar. In fact,

this makes substrate determination paramount to future work defining the role of QSOX1

in promotion of tumorigenesis since its most basic function is to contribute to the

structural fidelity of client proteins.

Using a combination of molecular and proteomic approaches, the mechanism by

which ebselen inhibits QSOX1 was determined. Ebselen has been observed to bind to

sulfhydryls and, in some instances, this is the reported mechanism of inhibition of

enzymatic activity [69]. Its binding forms a covalent bond between the sulfur atom in an

unpaired cysteine with the selenium moiety in ebselen [53]. Such a modification would

be expected to measurably increase the molecular mass of interacting partners of ebselen,

and it was thus hypothesized that ebselen interacted with the redox active cysteines in

rQSOX1, resulting in its inhibition. To probe this possibility, rQSOX1 was treated with

ebselen and subjected the protein to mass spectrometric analysis by LC-MS (Figure

11A). Increased mass of rQSOX1 treated with ebselen was observed (middle), compared

to vehicle-treated QSOX1 (top); this mass increase corresponded to the molecular weight

of exactly two molecules of ebselen binding to QSOX1. The identity of these cysteines

were determined, as this has important implications in the pharmacodynamics of ebselen

inhibition. Ammoinia-based cleavage of free cysteines following their labeling with 1-

Cyano-4-dimethylaminopyridinium tetrafluoroborate (CDAP) identified ebselen-binding

cysteines through molecular weight mapping of the cleaved products (Figure 12). This

approach identified C165 and C237 in native QSOX1 as those responsible for binding.

This result was surprising because these cysteines are not thought to participate in the

accepted disulfide relay pathway of QSOX1 [23]. Nonetheless, the identity of these

cysteines raised important questions worthy of further investigation: what, for example, is

the function (if any) of these cysteines in native QSOX1?  One possibility is that they

somehow participate in the QSOX1 reaction cycle and thus interrupt electron flow during

intramolecular disulfide transfer. While this is unlikely, these cysteines are highly

conserved in highly divergent taxa (Figure 16) suggesting, at least, that they may be

functional. More likely is another possibility. The Fass group has reported that a conformational change promotes the transfer of electrons between the thioredoxin and ERV domains, bringing their CXXC motifs into close proximity to facilitate this exchange [20, 21]. This conformational change is dependent on the flexible linker that exists between these domains, a predicted disordered region with no discrete secondary structure [26]; this region contains C165. We hypothesize that steric interruption of the proposed conformational change by ebselen binding to C165 may result in QSOX1 inhibition, but future studies are required to address this hypothesis.

A second small molecule screen identifying SBI-183 as a QSOX1 inhibitor was followed up with similar biological analyses of this molecule in tumor cell lines and *in vivo*. In renal cancer cell lines, SBI-183 was found to be highly active as evidenced by a dose response and kinetic data probing its growth inhibitory effects (Figures 19 and 20, respectively).

Similar to ebselen treatment and with QSOX1 knockdowns, SBI-183 inhibited the invasion of tumor cell lines in trans-well migration assays, belaboring the involvement of QSOX1 in this process (Figure 21). In nude mice bearing renal cell tumor xenografts, daily gavage of SBI-183 markedly decreased tumor growth (Figure 22). This result is particularly exciting with respect to UOK117 (Figure 22B), since the sarcomatoid lineage of renal cell carcinoma is highly aggressive and few therapeutic options exist [76]. It is worth noting, however, that ebselen was not active against this cell line *in vitro*, suggesting the need for additional research to clarify the role of both QSOX1 and these lead inhibitors on tumor cell growth.

Extracellular matrix modulation by QSOX1 promotes an invasive phenotype and has been implicated in discrete pro-invasive components into the ECM. Given the dynamic regulatory capacity of the ECM, targeting the ability of tumor cells to modulate its composition has the potential to retard the tumorigenic process [44, 46, 47, 93]. Since QSOX1 was shown to directly contribute to laminin α4 deposition and has other likely targets, we sought to determine whether QSOX1 inhibition led to defects in the ECM. Both ebselen and SBI-183 were found to decrease the ability of laminin α4 to properly assemble in the ECM and led to a general increase in the presence of extracellular sulfhydryls, highly suggestive of the presence of QSOX1 substrates (Figures 10 and 22, respectively). This result both strengthens the association between these molecules and the inhibition of QSOX1 activity in a biological system, they also suggest potential utility for exploring the cell biology of QSOX1 using these molecular probes.

It is clear from the results presented here that chemical inhibition of QSOX1 has enormous potential as an investigational therapeutic avenue. Future research should focus on the contribution of QSOX1 to metastasis *in vivo*. 90% of cancer deaths are caused by metastatic spread of tumors from the primary site [94]. Local invasion occurs prior to metastatic dissemination and is mediated, in part, by alteration of the extracellular matrix by tumor cells [95, 96]. Evidenced by the crucial role of QSOX1 to invasive processes described by multiple groups and by the results of this work showing its inhibition leads to a decrease in invasion, an *in vivo* metastatic model utilizing QSOX1 inhibitors is required.

The specificity of new inhibitors and those described here should also be explored, with an emphasis on the identification of new molecules through small molecule screening using defined biological substrates as well as the structural modulation of ebselen and SBI-183 (and new molecules) using rational design-based approaches like molecular modeling (reviewed in [97]). A more useful counterscreen should also be developed, such as the use of ALR and protein disulfide isomerase, since these proteins have similar biochemical activity to QSOX1 [27, 98, 99]. Molecules that preferably inhibit QSOX1 over structurally related enzymes is highly desirable. Such a screen may identify inhibitors that exploit the unique structural and biochemical characteristics of QSOX1. The identification and improvement of molecules that more specifically inhibit QSOX1 will yield superior biological insights and, in a clinical context, fewer off-target effects that may reduce toxicity and increase therapeutic value [100].

An extremely important avenue of future research involves the characterization of the intra- and extracellular substrates of QSOX1. While few protein substrates are currently known, their identities could reveal both novel biology and potential applictions to QSOX1 inhibition. Some research has been performed to identify substrates in a broad sense [28, 101], but the specific identification of discrete substrates by mass spectrometry would yield enormous insight into the role of QSOX1 in normal and pathological processes. This could be very simply accomplished in a number of ways. For example, one could take advantage of the increased sulfhydryls that result from QSOX1

knockdown and inhibition, label them with maleimide conjugated to biotin, trypsin

digest, and affinity purify the labeled substrate peptides for mass spectrometric analysis.

The results of this research provide proof-of-principle that the enzymatic

inhibition of QSOX1 has potential therapeutic utility. Decreased growth and invasion in

tumor cells, extracellular matrix modulation, and the *in vivo* activity of QSOX1 inhibitory

compounds is a crucial first step into investigating QSOX1 as a true clinical target. With

the limited number of targeted therapies currently available to physicians and the general

lack of compounds that target invasive behavior, building on the work here may have the

potential to save lives.

REFERENCES

1.      Sevier CS, Kaiser CA: **Ero1 and redox homeostasis in the endoplasmic reticulum.** *Biochimica et biophysica acta* 2008, **1783:**549-556.

2.      Feige MJ, Hendershot LM: **Disulfide bonds in ER protein folding and homeostasis.** *Current opinion in cell biology* 2011, **23:**167-175.

3.      Lopez-Mirabal HR, Winther JR: **Redox characteristics of the eukaryotic cytosol.** *Biochimica et biophysica acta* 2008, **1783:**629-640.

4.      Saaranen MJ, Ruddock LW: **Disulfide bond formation in the cytoplasm.** *Antioxidants & redox signaling* 2013, **19:**46-53.

5.      Riemer J, Bulleid N, Herrmann JM: **Disulfide formation in the ER and mitochondria: two solutions to a common process.** *Science* 2009, **324:**1284-1287.

6.      Tu BP, Weissman JS: **The FAD- and O(2)-dependent reaction cycle of Ero1-mediated oxidative protein folding in the endoplasmic reticulum.** *Molecular cell* 2002, **10:**983-994.

7.      Gross E, Sevier CS, Heldman N, Vitu E, Bentzur M, Kaiser CA, Thorpe C, Fass D: **Generating disulfides enzymatically: reaction products and electron acceptors of the endoplasmic reticulum thiol oxidase Ero1p.** *Proceedings of the National Academy of Sciences of the United States of America* 2006, **103:**299-304.

8.      Freedman RB: **The formation of protein disulphide bonds.** *Current opinion in structural biology* 1995, **5:**85-91.

9.      Wittke I, Wiedemeyer R, Pillmann A, Savelyeva L, Westermann F, Schwab M: **Neuroblastoma-derived sulfhydryl oxidase, a new member of the sulfhydryl oxidase/Quiescin6 family, regulates sensitization to interferon gamma-induced cell death in human neuroblastoma cells.** *Cancer research* 2003, **63:**7742-7752.

10.     Coppock DL, Cina-Poppe D, Gilleran S: **The quiescin Q6 gene (QSCN6) is a fusion of two ancient gene families: thioredoxin and ERV1.** *Genomics* 1998, **54:**460-468.

11.     Lisowsky T, Lee JE, Polimeno L, Francavilla A, Hofhaus G: **Mammalian augmenter of liver regeneration protein is a sulfhydryl oxidase.** *Digestive and liver disease : official journal of the Italian Society of Gastroenterology and the Italian Association for the Study of the Liver* 2001, **33:**173-180.

12.    Fass D: **The Erv family of sulfhydryl oxidases.** *Biochimica et biophysica acta* 2008, **1783:**557-566.

13.    Kodali VK, Thorpe C: **Quiescin sulfhydryl oxidase from Trypanosoma brucei: catalytic activity and mechanism of a QSOX family member with a single thioredoxin domain.** *Biochemistry* 2010, **49:**2075-2085.

14.    Alon A, Heckler EJ, Thorpe C, Fass D: **QSOX contains a pseudo-dimer of functional and degenerate sulfhydryl oxidase domains.** *FEBS letters* 2010, **584:**1521-1525.

15.    Rudolf J, Pringle MA, Bulleid NJ: **Proteolytic processing of QSOX1A ensures efficient secretion of a potent disulfide catalyst.** *The Biochemical journal* 2013, **454:**181-190.

16.    Hoober KL, Joneja B, White HB, 3rd, Thorpe C: **A sulfhydryl oxidase from chicken egg white.** *The Journal of biological chemistry* 1996, **271:**30510-30516.

17.    Hoober KL, Glynn NM, Burnside J, Coppock DL, Thorpe C: **Homology between egg white sulfhydryl oxidase and quiescin Q6 defines a new class of flavin-linked sulfhydryl oxidases.** *The Journal of biological chemistry* 1999, **274:**31759-31762.

18.    Coppock D, Kopman C, Gudas J, Cina-Poppe DA: **Regulation of the quiescence-induced genes: quiescin Q6, decorin, and ribosomal protein S29.** *Biochemical and biophysical research communications* 2000, **269:**604-610.

19.    Chakravarthi S, Jessop CE, Willer M, Stirling CJ, Bulleid NJ: **Intracellular catalysis of disulfide bond formation by the human sulfhydryl oxidase, QSOX1.** *The Biochemical journal* 2007, **404:**403-411.

20.    Alon A, Grossman I, Gat Y, Kodali VK, DiMaio F, Mehlman T, Haran G, Baker D, Thorpe C, Fass D: **The dynamic disulphide relay of quiescin sulphydryl oxidase.** *Nature* 2012, **488:**414-418.

21.    Gat Y, Vardi-Kilshtain A, Grossman I, Major DT, Fass D: **Enzyme structure captures four cysteines aligned for disulfide relay.** *Protein science : a publication of the Protein Society* 2014, **23:**1102-1112.

22.    Grossman I, Alon A, Ilani T, Fass D: **An inhibitory antibody blocks the first step in the dithiol/disulfide relay mechanism of the enzyme QSOX1.** *Journal of molecular biology* 2013, **425:**4366-4378.

23.     Heckler EJ, Alon A, Fass D, Thorpe C: **Human quiescin-sulfhydryl oxidase, QSOX1: probing internal redox steps by mutagenesis.** *Biochemistry* 2008, **47:**4955-4963.

24.     Israel BA, Kodali VK, Thorpe C: **Going through the barrier: coupled disulfide exchange reactions promote efficient catalysis in quiescin sulfhydryl oxidase.** *The Journal of biological chemistry* 2014, **289:**5274-5284.

25.     Raje S, Glynn NM, Thorpe C: **A continuous fluorescence assay for sulfhydryl oxidase.** *Analytical biochemistry* 2002, **307:**266-272.

26.     Raje S, Thorpe C: **Inter-domain redox communication in flavoenzymes of the quiescin/sulfhydryl oxidase family: role of a thioredoxin domain in disulfide bond formation.** *Biochemistry* 2003, **42:**4560-4568.

27.     Rancy PC, Thorpe C: **Oxidative protein folding in vitro: a study of the cooperation between quiescin-sulfhydryl oxidase and protein disulfide isomerase.** *Biochemistry* 2008, **47:**12047-12056.

28.     Zheng W, Chu Y, Yin Q, Xu L, Yang C, Zhang W, Tang Y, Yang Y: **Crucial effect of the first CXXC motif of human QSOX 1b on the activity to different substrates.** *Journal of biochemistry* 2011, **149:**293-300.

29.     Zheng W, Zhang W, Hu W, Zhang C, Yang Y: **Exploring the smallest active fragment of HsQSOX1b and finding a highly efficient oxidative engine.** *PLoS One* 2012, **7:**e40935.

30.     Morel C, Adami, P., Musard, J. F., Duval, D., Radom, J., Jouvenot, M.: **Involvement of sulfhydryl oxidase QSOX1 in the protection of cells against oxidative stress-induced apoptosis.** *Exp Cell Res* 2007, **313:**3971-3982.

31.     Song H, Zhang B, Watson MA, Humphrey PA, Lim H, Milbrandt J: **Loss of Nkx3.1 leads to the activation of discrete downstream target genes during prostate tumorigenesis.** *Oncogene* 2009, **28:**3307-3319.

32.     Antwi K, Hostetter G, Demeure M, Decker G, Ruiz Y, Sielaff T, Koep L, Lake D: **Analysis of Human Plasma Peptidome Reveals Potential Biomarker for Pancreatic Cancer.** *J Proteome Res* 2009, **8:**4722-4731.

33.     Antwi K, Hostetter G, Demeure MJ, Katchman BA, Decker GA, Ruiz Y, Sielaff TD, Koep LJ, Lake DF: **Analysis of the plasma peptidome from pancreas cancer patients connects a peptide in plasma to overexpression of the parent protein in tumors.** *Journal of proteome research* 2009, **8:**4722-4731.

34.     Hanahan D, Weinberg RA: **The hallmarks of cancer.** *Cell* 2000, **100:**57-70.

35.     Katchman BA, Antwi K, Hostetter G, Demeure MJ, Watanabe A, Decker GA, Miller LJ, Von Hoff DD, Lake DF: **Quiescin sulfhydryl oxidase 1 promotes invasion of pancreatic tumor cells mediated by matrix metalloproteinases.** *Molecular cancer research : MCR* 2011, **9:**1621-1631.

36.     Zheng H, Takahashi H, Murai Y, Cui Z, Nomoto K, Niwa H, Tsuneyama K, Takano Y: **Expressions of MMP-2, MMP-9 and VEGF are closely linked to growth, invasion, metastasis and angiogenesis of gastric carcinoma.** *Anticancer research* 2006, **26:**3579-3583.

37.     Shi CY, Fan Y, Liu B, Lou WH: **HIF1 contributes to hypoxia-induced pancreatic cancer cells invasion via promoting QSOX1 expression.** *Cellular physiology and biochemistry : international journal of experimental cellular physiology, biochemistry, and pharmacology* 2013, **32:**561-568.

38.     Katchman BA, Ocal IT, Cunliffe HE, Chang YH, Hostetter G, Watanabe A, Lobello J, Lake DF: **Expression of quiescin sulfhydryl oxidase 1 is associated with a highly invasive phenotype and correlates with a poor prognosis in Luminal B breast cancer.** *Breast cancer research : BCR* 2013, **15:**R28.

39.     Soloviev M, Esteves MP, Amiri F, Crompton MR, Rider CC: **Elevated transcription of the gene QSOX1 encoding quiescin Q6 sulfhydryl oxidase 1 in breast cancer.** *PloS one* 2013, **8:**e57327.

40.     Pernodet N, Hermetet F, Adami P, Vejux A, Descotes F, Borg C, Adams M, Pallandre JR, Viennet G, Esnard F, et al: **High expression of QSOX1 reduces tumorogenesis, and is associated with a better outcome for breast cancer patients.** *Breast cancer research : BCR* 2012, **14:**R136.

41.     Das P, Siegers GM, Postovit LM: **Illuminating luminal B: QSOX1 as a subtype-specific biomarker.** *Breast cancer research : BCR* 2013, **15:**104.

42.     Gattazzo F, Urciuolo A, Bonaldo P: **Extracellular matrix: a dynamic microenvironment for stem cell niche.** *Biochimica et biophysica acta* 2014, **1840:**2506-2519.

43.     Xu R, Boudreau A, Bissell MJ: **Tissue architecture and function: dynamic reciprocity via extra- and intra-cellular matrices.** *Cancer metastasis reviews* 2009, **28:**167-176.

44.     Pickup MW, Mouw JK, Weaver VM: **The extracellular matrix modulates the hallmarks of cancer.** *EMBO reports* 2014, **15:**1243-1253.

45.     Ilani T, Alon A, Grossman I, Horowitz B, Kartvelishvily E, Cohen SR, Fass D: **A secreted disulfide catalyst controls extracellular matrix composition and function.** *Science* 2013, **341:**74-76.

46.     Nagato S, Nakagawa K, Harada H, Kohno S, Fujiwara H, Sekiguchi K, Ohue S, Iwata S, Ohnishi T: **Downregulation of laminin alpha4 chain expression inhibits glioma invasion in vitro and in vivo.** *International journal of cancer Journal international du cancer* 2005, **117:**41-50.

47.     Vainionpaa N, Lehto VP, Tryggvason K, Virtanen I: **Alpha4 chain laminins are widely expressed in renal cell carcinomas and have a de-adhesive function.** *Laboratory investigation; a journal of technical methods and pathology* 2007, **87:**780-791.

48.     Hanavan PD, Borges CR, Katchman BA, Faigel DO, Ho TH, Ma CT, Sergienko EA, Meurice N, Petit JL, Lake DF: **Ebselen inhibits QSOX1 enzymatic activity and suppresses invasion of pancreatic and renal cancer cell lines.** *Oncotarget* 2015, **6:**18418-18428.

49.     Sapra A, Ramadan D, Thorpe C: **Multivalency in the inhibition of oxidative protein folding by arsenic(III) species.** *Biochemistry* 2015, **54:**612-621.

50.     Tomayko MM, Reynolds CP: **Determination of subcutaneous tumor size in athymic (nude) mice.** *Cancer chemotherapy and pharmacology* 1989, **24:**148-154.

51.     Raje S, Glynn NM, Thorpe C: **A continuous fluorescence assay for sulfhydryl oxidase.** *Anal Biochem* 2002, **307:**266-272.

52.     Wu J, Gage DA, Watson JT: **A strategy to locate cysteine residues in proteins by specific chemical cleavage followed by matrix-assisted laser desorption/ionization time-of-flight mass spectrometry.** *Anal Biochem* 1996, **235:**161-174.

53.     Schewe T: **Molecular actions of ebselen--an antiinflammatory antioxidant.** *General pharmacology* 1995, **26:**1153-1169.

54.     Wu J, Gage DA, Watson JT: **A strategy to locate cysteine residues in proteins by specific chemical cleavage followed by matrix-assisted laser desorption/ionization time- of-flight mass spectrometry.** *Anal Biochem* 1996, **235:**161-174.

55.     Wu J, Watson JT: **A novel methodology for assignment of disulfide bond pairings in proteins.** *Protein Science* 1997, **6:**391-398.

56.     Sato AK, Sexton, D. J., Morganelli, L. A., Cohen, E. H., Wu, Q. L., Conley, G. P., Streltsova, Z., Lee, S. W., Devlin, M., DeOliveira, D. B., Enright, J., Kent, R. B., Wescott, C. R., Ransohoff, T. C., Ley, A. C., and Ladner, R. C.: **Development of mammalian serum albumin affinity purification media by peptide phage display.** *Biotechnol Prog* 2002, **18:**182–192.

57.     Wu J, Yang Y, Watson JT: **Trapping of intermediates during the refolding of recombinant human epidermal growth factor (hEGF) by cyanylation, and subsequent structural elucidation by mass spectrometry.** *Protein Science* 1998, **7:**1017-1028.

58.     Wohlfahrt G, Trivic S, Zeremski J, Pericin D, Leskovac V: **The chemical mechanism of action of glucose oxidase from Aspergillus niger.** *Molecular and cellular biochemistry* 2004, **260:**69-83.

59.     Ogawa A, Yoshimoto T, Kikuchi H, Sano K, Saito I, Yamaguchi T, Yasuhara H: **Ebselen in acute middle cerebral artery occlusion: a placebo-controlled, double-blind clinical trial.** *Cerebrovasc Dis* 1999, **9:**112-118.

60.     Saito I, Asano T, Sano K, Takakura K, Abe H, Yoshimoto T, Kikuchi H, Ohta T, Ishibashi S: **Neuroprotective effect of an antioxidant, ebselen, in patients with delayed neurological deficits after aneurysmal subarachnoid hemorrhage.** *Neurosurgery* 1998, **42:**269-277; discussion 277-268.

61.     Yamaguchi T, Sano K, Takakura K, Saito I, Shinohara Y, Asano T, Yasuhara H: **Ebselen in acute ischemic stroke: a placebo-controlled, double-blind clinical trial. Ebselen Study Group.** *Stroke; a journal of cerebral circulation* 1998, **29:**12-17.

62.     Muller A, Cadenas E, Graf P, Sies H: **A novel biologically active seleno-organic compound--I. Glutathione peroxidase-like activity in vitro and antioxidant capacity of PZ 51 (Ebselen).** *Biochemical pharmacology* 1984, **33:**3235-3239.

63.     Wendel A, Fausel M, Safayhi H, Tiegs G, Otter R: **A novel biologically active seleno-organic compound--II. Activity of PZ 51 in relation to glutathione peroxidase.** *Biochemical pharmacology* 1984, **33:**3241-3245.

64.     Parnham MJ, Kindt S: **A novel biologically active seleno-organic compound--III. Effects of PZ 51 (Ebselen) on glutathione peroxidase and secretory activities of mouse macrophages.** *Biochemical pharmacology* 1984, **33:**3247-3250.

65.     Parnham MJ, Leyck S, Graf E, Dowling EJ, Blake DR: **The pharmacology of ebselen.** *Agents and actions* 1991, **32:**4-9.

66.     Wagner G, Schuch G, Akerboom TP, Sies H: **Transport of ebselen in plasma and its transfer to binding sites in the hepatocyte.** *Biochemical pharmacology* 1994, **48:**1137-1144.

67.     Sies H: **Ebselen, a selenoorganic compound as glutathione peroxidase mimic.** *Free radical biology & medicine* 1993, **14:**313-323.

68.     Terentis AC, Freewan M, Sempertegui Plaza TS, Raftery MJ, Stocker R, Thomas SR: **The selenazal drug ebselen potently inhibits indoleamine 2,3-dioxygenase by targeting enzyme cysteine residues.** *Biochemistry* 2010, **49:**591-600.

69.     Zembowicz A, Hatchett RJ, Radziszewski W, Gryglewski RJ: **Inhibition of endothelial nitric oxide synthase by ebselen. Prevention by thiols suggests the inactivation by ebselen of a critical thiol essential for the catalytic activity of nitric oxide synthase.** *The Journal of pharmacology and experimental therapeutics* 1993, **267:**1112-1118.

70.     Heckler EJ, Rancy PC, Kodali VK, Thorpe C: **Generating disulfides with the Quiescin-sulfhydryl oxidases.** *Biochimica et biophysica acta* 2008, **1783:**567-577.

71.     Wood ZA, Poole LB, Karplus PA: **Peroxiredoxin evolution and the regulation of hydrogen peroxide signaling.** *Science* 2003, **300:**650-653.

72.     Larkin MA, Blackshields G, Brown NP, Chenna R, McGettigan PA, McWilliam H, Valentin F, Wallace IM, Wilm A, Lopez R, et al: **Clustal W and Clustal X version 2.0.** *Bioinformatics* 2007, **23:**2947-2948.

73.     Lake DF, Faigel DO: **The Emerging Role of QSOX1 in Cancer.** *Antioxidants & redox signaling* 2014.

74.     McCubrey JA, Steelman LS, Chappell WH, Abrams SL, Wong EW, Chang F, Lehmann B, Terrian DM, Milella M, Tafuri A, et al: **Roles of the Raf/MEK/ERK pathway in cell growth, malignant transformation and drug resistance.** *Biochimica et biophysica acta* 2007, **1773:**1263-1284.

75.     Borges BE, Appel MH, Cofre AR, Prado ML, Steclan CA, Esnard F, Zanata SM, Laurindo FR, Nakao LS: **The flavo-oxidase QSOX1 supports vascular smooth muscle cell migration and proliferation: Evidence for a role in neointima growth.** *Biochimica et biophysica acta* 2015, **1852:**1334-1346.

76.     Mian BM, Bhadkamkar N, Slaton JW, Pisters PW, Daliani D, Swanson DA, Pisters LL: **Prognostic factors and survival of patients with sarcomatoid renal cell carcinoma.** *The Journal of urology* 2002, **167:**65-70.
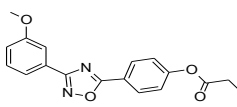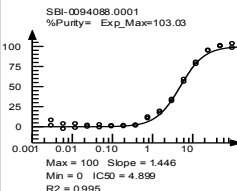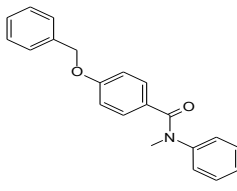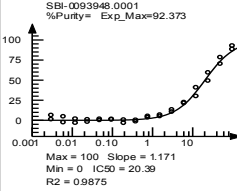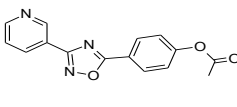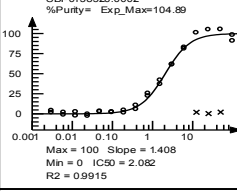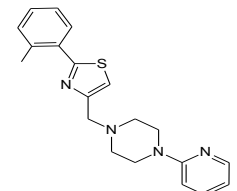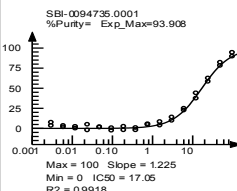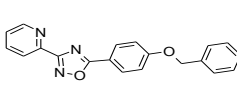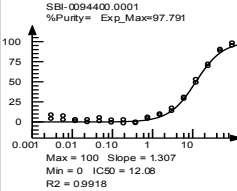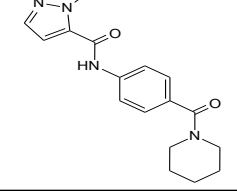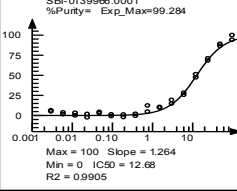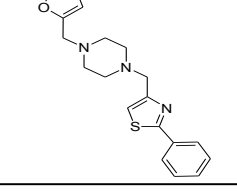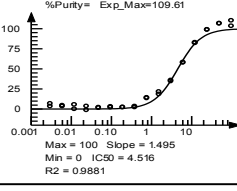
77.    Kroeger N, Seligson DB, Signoretti S, Yu H, Magyar CE, Huang J, Belldegrun AS, Pantuck AJ: **Poor prognosis and advanced clinicopathological features of clear cell renal cell carcinoma (ccRCC) are associated with cytoplasmic subcellular localisation of Hypoxia inducible factor-2alpha.** *European journal of cancer* 2014, **50:**1531-1540.

78.    Liu Y, Gray NS: **Rational design of inhibitors that bind to inactive kinase conformations.** *Nature chemical biology* 2006, **2:**358-364.

79.    Rice RL, Rusnak JM, Yokokawa F, Yokokawa S, Messner DJ, Boynton AL, Wipf P, Lazo JS: **A targeted library of small-molecule, tyrosine, and dual-specificity phosphatase inhibitors derived from a rational core design and random side chain variation.** *Biochemistry* 1997, **36:**15965-15974.

80.    Azad GK, Tomar RS: **Ebselen, a promising antioxidant drug: mechanisms of action and targets of biological pathways.** *Mol Biol Rep* 2014.

81.    Siegal GP, Barsky SH, Terranova VP, Liotta LA: **Stages of neoplastic transformation of human breast tissue as monitored by dissolution of basement membrane components. An immunoperoxidase study.** *Invasion & metastasis* 1981, **1:**54-70.

82.    Hunter KW, Crawford NP, Alsarraj J: **Mechanisms of metastasis.** *Breast cancer research : BCR* 2008, **10 Suppl 1:**S2.

83.    Bissig H, Richter J, Desper R, Meier V, Schraml P, Schaffer AA, Sauter G, Mihatsch MJ, Moch H: **Evaluation of the clonal relationship between primary and metastatic renal cell carcinoma by comparative genomic hybridization.** *The American journal of pathology* 1999, **155:**267-274.

84.    Kuukasjarvi T, Karhu R, Tanner M, Kahkonen M, Schaffer A, Nupponen N, Pennanen S, Kallioniemi A, Kallioniemi OP, Isola J: **Genetic heterogeneity and clonal evolution underlying development of asynchronous metastasis in human breast cancer.** *Cancer research* 1997, **57:**1597-1604.

85.    Schmidt-Kittler O, Ragg T, Daskalakis A, Granzow M, Ahr A, Blankenstein TJ, Kaufmann M, Diebold J, Arnholdt H, Muller P, et al: **From latent disseminated cells to overt metastasis: genetic analysis of systemic breast cancer progression.** *Proceedings of the National Academy of Sciences of the United States of America* 2003, **100:**7737-7742.

86.    Kaplan RN, Rafii S, Lyden D: **Preparing the "soil": the premetastatic niche.** *Cancer research* 2006, **66:**11089-11093.

87.    Paget S: **The distribution of secondary growths in cancer of the breast. 1889.** *Cancer metastasis reviews* 1989, **8:**98-101.

88. Psaila B, Lyden D: **The metastatic niche: adapting the foreign soil.** *Nature reviews Cancer* 2009, **9:**285-293.

89. Thiery JP: **Epithelial-mesenchymal transitions in tumour progression.** *Nature reviews Cancer* 2002, **2:**442-454.

90. Karnoub AE, Dash AB, Vo AP, Sullivan A, Brooks MW, Bell GW, Richardson AL, Polyak K, Tubo R, Weinberg RA: **Mesenchymal stem cells within tumour stroma promote breast cancer metastasis.** *Nature* 2007, **449:**557-563.

91. Mani SA, Guo W, Liao MJ, Eaton EN, Ayyanan A, Zhou AY, Brooks M, Reinhard F, Zhang CC, Shipitsin M, et al: **The epithelial-mesenchymal transition generates cells with properties of stem cells.** *Cell* 2008, **133:**704-715.

92. Hurt EM, Farrar WL: **Cancer stem cells: the seeds of metastasis?** *Molecular interventions* 2008, **8:**140-142.

93. Tran M, Rousselle P, Nokelainen P, Tallapragada S, Nguyen NT, Fincher EF, Marinkovich MP: **Targeting a tumor-specific laminin domain critical for human carcinogenesis.** *Cancer Res* 2008, **68:**2885-2894.

94. Mehlen P, Puisieux A: **Metastasis: a question of life or death.** *Nature reviews Cancer* 2006, **6:**449-458.

95. Wolf K, Wu YI, Liu Y, Geiger J, Tam E, Overall C, Stack MS, Friedl P: **Multi-step pericellular proteolysis controls the transition from individual to collective cancer cell invasion.** *Nature cell biology* 2007, **9:**893-904.

96. Timpson P, Serrels A, Canel M, Frame MC, Brunton VG, Anderson KI: **Quantitative real-time imaging of molecular dynamics during cancer cell invasion and metastasis in vivo.** *Cell adhesion & migration* 2009, **3:**351-354.

97. Lin JH: **Review structure- and dynamics-based computational design of anticancer drugs.** *Biopolymers* 2016, **105:**2-9.

98. Araki K, Inaba K: **Structure, mechanism, and evolution of Ero1 family enzymes.** *Antioxidants & redox signaling* 2012, **16:**790-799.

99. Sztolsztener ME, Brewinska A, Guiard B, Chacinska A: **Disulfide bond formation: sulfhydryl oxidase ALR controls mitochondrial biogenesis of human MIA40.** *Traffic* 2013, **14:**309-320.

100. Rudmann DG: **On-target and off-target-based toxicologic effects.** *Toxicologic pathology* 2013, **41:**310-314.
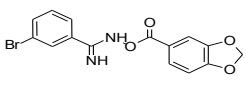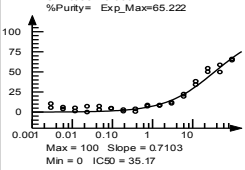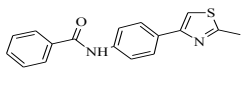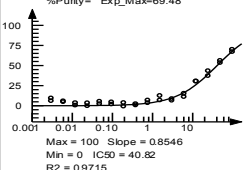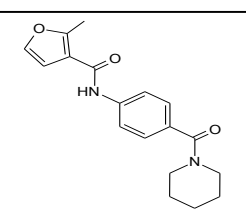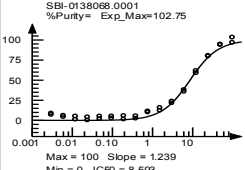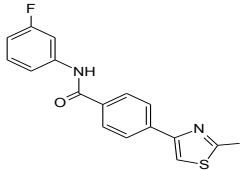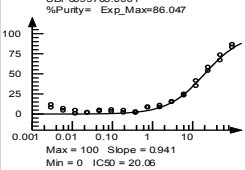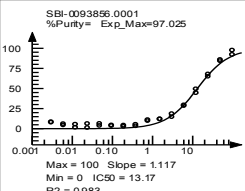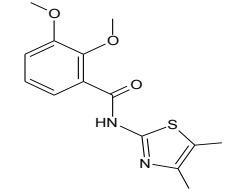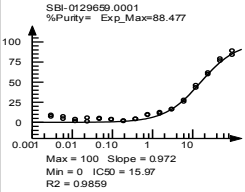
101. Codding JA, Israel BA, Thorpe C: **Protein substrate discrimination in the quiescin sulfhydryl oxidase (QSOX) family.** *Biochemistry* 2012, **51:**4226-4235.

APPENDIX A

INHIBITION DATA FROM SMALL MOLECULE SCREENS

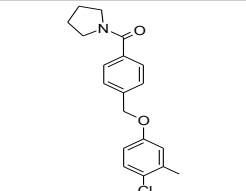| CompoundID | BatchID | Structure | QSOX1 IC50 (uM) | Error | ResponseCurve | Hill Coefficient |
|---|---|---|---|---|---|---|
| SBI-0094088 | SBI-0094088.0001 | | 4.89 | 0.2 | SBI-0094088.0001 %Purity= Exp_Max=103.03 Max = 100 Slope = 1.446 Min = 0 IC50 = 4.899 R2 = 0.995 | 1.5 |
| SBI-0093948 | SBI-0093948.0001 | | 20.3 | 0.9 | SBI-0093948.0001 %Purity= Exp_Max=92.373 Max = 100 Slope = 1.171 Min = 0 IC50 = 20.39 R2 = 0.9875 | 1.2 |
| SBI-0138526 | SBI-0138526.0002 | | 2.08 | 0.1 | SBI-0138526.0002 %Purity= Exp_Max=104.89 Max = 100 Slope = 1.408 Min = 0 IC50 = 2.082 R2 = 0.9915 | 1.4 |
| SBI-0094735 | SBI-0094735.0001 | | 17.0 | 0.6 | SBI-0094735.0001 %Purity= Exp_Max=93.908 Max = 100 Slope = 1.225 Min = 0 IC50 = 17.05 R2 = 0.9918 | 1.2 |
| SBI-0094400 | SBI-0094400.0001 | | 12.0 | 0.5 | SBI-0094400.0001 %Purity= Exp_Max=97.791 Max = 100 Slope = 1.307 Min = 0 IC50 = 12.08 R2 = 0.9918 | 1.3 |
| SBI-0139966 | SBI-0139966.0001 | | 12.6 | 0.5 | SBI-0139966.0001 %Purity= Exp_Max=99.284 Max = 100 Slope = 1.264 Min = 0 IC50 = 12.68 R2 = 0.9905 | 1.3 |
| SBI-0127912 | SBI-0127912.0001 | | 4.51 | 0.2 | SBI-0127912.0001 %Purity= Exp_Max=109.61 Max = 100 Slope = 1.495 Min = 0 IC50 = 4.516 R2 = 0.9881 | 1.5 |

| | | | | | | |
|---|---|---|---|---|---|---|
| SBI-0094401 | SBI-0094401.0001 | | 6.66 | 0.3 | SBI-0094401.0001<br>%Purity= Exp_Max=101.07<br>Max = 100 Slope = 1.39<br>Min = 0 IC50 = 6.668<br>R2 = 0.9925 | 1.4 |
| SBI-0143343 | SBI-0143343.0002 | | 11.7 | 0.5 | SBI-0143343.0002<br>%Purity= Exp_Max=92.919<br>Max = 100 Slope = 1.037<br>Min = 0 IC50 = 11.79<br>R2 = 0.992 | 1.0 |
| SBI-0088453 | SBI-0088453.0001 | | 6.80 | 0.3 | SBI-0088453.0001<br>%Purity= Exp_Max=103.38<br>Max = 100 Slope = 1.221<br>Min = 0 IC50 = 6.803<br>R2 = 0.9915 | 1.2 |
| SBI-0143183 | SBI-0143183.0002 | | 12.3 | 0.6 | SBI-0143183.0002<br>%Purity= Exp_Max=91.942<br>Max = 100 Slope = 1.052<br>Min = 0 IC50 = 12.34<br>R2 = 0.9893 | 1.1 |
| SBI-0137402 | SBI-0137402.0001 | | 19.1 | 1.0 | SBI-0137402.0001<br>%Purity= Exp_Max=87.836<br>Max = 100 Slope = 1.049<br>Min = 0 IC50 = 19.16<br>R2 = 0.9836 | 1.1 |
| SBI-0125703 | SBI-0125703.0001 | | 17.6 | 0.9 | SBI-0125703.0001<br>%Purity= Exp_Max=89.519<br>Max = 100 Slope = 1.057<br>Min = 0 IC50 = 17.65<br>R2 = 0.9853 | 1.1 |
| SBI-0132719 | SBI-0132719.0001 | | 5.32 | 0.3 | SBI-0132719.0001<br>%Purity= Exp_Max=105.57<br>Max = 100 Slope = 1.422<br>Min = 0 IC50 = 5.325<br>R2 = 0.9861 | 1.4 |

| SBI-0093213 | SBI-0093213.0001 |  | 35.1 | 3.1 | SBI-0093213.0001 %Purity= Exp_Max=65.222 <br> Max = 100 Slope = 0.7103 <br> Min = 0 IC50 = 35.17 <br> R2 = 0.9589 | 0.7 |
| SBI-0035734 | SBI-0035734.0001 |  | 40.8 | 2.6 | SBI-0035734.0001 %Purity= Exp_Max=69.48 <br> Max = 100 Slope = 0.8546 <br> Min = 0 IC50 = 40.82 <br> R2 = 0.9715 | 0.9 |
| SBI-0138068 | SBI-0138068.0001 |  | 8.59 | 0.5 | SBI-0138068.0001 %Purity= Exp_Max=102.75 <br> Max = 100 Slope = 1.239 <br> Min = 0 IC50 = 8.593 <br> R2 = 0.9867 | 1.2 |
| SBI-0099708 | SBI-0099708.0001 |  | 20.0 | 1.2 | SBI-0099708.0001 %Purity= Exp_Max=86.047 <br> Max = 100 Slope = 0.941 <br> Min = 0 IC50 = 20.06 <br> R2 = 0.9799 | 0.9 |
| SBI-0093856 | SBI-0093856.0001 |  | 13.1 | 0.7 | SBI-0093856.0001 %Purity= Exp_Max=97.025 <br> Max = 100 Slope = 1.117 <br> Min = 0 IC50 = 13.17 <br> R2 = 0.983 | 1.1 |
| SBI-0129659 | SBI-0129659.0001 |  | 15.9 | 0.8 | SBI-0129659.0001 %Purity= Exp_Max=88.477 <br> Max = 100 Slope = 0.972 <br> Min = 0 IC50 = 15.97 <br> R2 = 0.9859 | 1.0 |

**Table 1**. Raw data from small molecule screen of rQSOX1 against Sanford Burnham Prebys Medical Discovery Institute 50,000 compound library.